*Jimmie C. Oxley,[1] Ph.D.; James L. Smith,[1] Ph.D.; Elmo Resende,[2] M.S.; Evan Rogers,[1] B.S.; Richard A. Strobel,[3] B.S.; and Edward C. Bender,[3] B.S.*

# Improvised Explosive Devices: Pipe Bombs*

**REFERENCE:** Oxley JC, Smith JL, Resende E, Rogers E, Strobel RA, Bender EC. Improvised explosive devices: pipe bombs. J Forensic Sci 2001;46(3):510–534.

**ABSTRACT:** The fragments from 56 pipe bombs were collected (average recovery 87%), counted, weighed, sorted, and photographed. The matrix examined included eight energetic fillers, two initiation systems, three types of pipe, and several degrees of fill. The matrix and results are summarized in Table 1. For identical devices, the overall fragmentation pattern was surprisingly reproducible. The fragmentation patterns are presented in photos, but they are also reduced to numerical evaluators. A particularly useful evaluator is the fragment weight distribution map (FWDM) which describes explosive power with a single variable—the slope. This value is independent of device size and percent recovery. We believe this database of 56 pipe bombs is the largest controlled study of these devices. This study demonstrates the possibility that, even in circumstances where chemical residue cannot be found, sufficient evidence is present in the pipe fragments to identify the nature of the energetic filler.

**KEYWORDS:** forensic science, pipe bomb, improvised explosive devices, fragmentation, smokeless powder, black powder

Of the improvised explosive devices used in illegal activity in the United States, pipe bombs are a dominant configuration. Over the five year period of 1993 to 1997 ATF reported over 10 000 bombings or attempted bombings. In terms of containment of the explosive, pipes make up 34% and bottles 53% (1). In terms of explosive filler, flammable liquids make up 30%, black powder 10%, smokeless powder 8%, photo and fireworks powders 17%, matchheads 2%, and unspecified chemicals 26% (1). If flammable liquid devices are removed from the statistics, the percentage of devices that are pipe bombs is greater than 60% (2). Although pipe bombs are frequently used to kill or maim, (e.g., the UNABOMBER devices, the device at the Atlanta Olympics, and the devices at Littleton, CO), to date, little has been done to document their blast characteristics and effects. The data presented herein represents a controlled study documenting and characterizing pipe bombs under various conditions. It is hoped this study will be useful for forensic investigations, training of crime scene personnel, and the documentation of the observable blast effects for court evidence. The objective is to understand the correlation between damage to the pipe and its size, energetic filler, initiation system, and quantity of energetic material. Specifically, the goal is to sufficiently characterize pipe bomb fragmentation so that the device can be reconstructed (at least on paper) even without the discovery of chemical residue.

[1] Chemistry Department, University of Rhode Island, Kingston, RI.
[2] Graduate student with partial support from the CNPq, Brazil and Judiciary Police of Brazil, Chemistry Department, University of Rhode Island, Kingston, RI.
[3] Bureau of Alcohol, Tobacco, & Firearms, Forensic Science Laboratory-Washington, Rockville, MD.
* The bulk of this project was supported by TSWG with a grant through ONR 000149611095. Funding for four tests was provided by the URI Forensic Science Partnership.
Received 26 May 2000; and in revised form 19 July 2000; accepted 21 July 2000.

## Experimental Protocol

The effects of a number of variables on device performance were examined by initiating 56 pipe bombs, two of which were blanks. Table 1, with pipes grouped by energetic filler, shows some of the results. All pipes were detonated in 55 gal steel drums filled with sand (pipes 1–37) or Grit-o-Cob® (pipes 38–56) to protect and capture the thrown pipe fragments. For upright pipes, sand only touched the bottom end cap of the pipe. The rest of the pipe was isolated from the sand by a 12 in. cylindrical cardboard sleeve 8 in. in diameter. The two types of initiators used were a #12 detonator or an electric squib. The initiator was placed at one end of the pipe. For the upright tests, the initiator end was at the top. For the first 37 pipes, fragments were collected (by sieve and magnet), washed with water, dried, and stored in sealed plastic bags. For pipes 38–56, fragments were not washed with water, but some were immediately immersed in methanol to prevent rust. Once samples were returned to the laboratory they were counted, weighed, and sorted as to origin (i.e., pipe or end cap). Data was plotted in fragment weight distribution maps (FWDMs) and added to the pipe bomb database. The visual appearance of the fragments was described and photographed.

Most pipe bombs (51) were constructed of schedule 40, galvanized steel, butt-end welded pipes. A few pipes were made of PVC (2) or galvanized, seamless steel (3). Pipe dimensions were 1 in. by 6 in. (14), 2 in. by 12 in. (31), 2.5 in. by 15 in. (5), and 1.5 in. by 12 in (6) with energetic material weight ranging from 0.5 to 2 lbs. In most tests the length to diameter (L/D) ratio was set at 6/1; this was considered long enough to allow build-up to detonation. Eight different energetic fills, both double-base (DB) and single-base (SB), were chosen to represent a variety of deflagration/detonation characteristics: black powder (7); WC 870 (DB) (5); IMR-PB (SB) (6); Red Dot (DB) (16); chlorate/aluminum paint (1); Winchester Action Pistol (DB) (2); Bullseye (DB) (15); and nitromethane (2). Nitromethane ($MeNO_2$) was chosen as the standard by which to compare other energetic fills because it is highly explosive with well-characterized performance. When sensitized with 10% diethylenetriamine, nitromethane is cap-sensitive and can produce a blast wave greater than an equivalent amount of TNT (TNT equivalancy ~1.1). Table 1 shows the test matrixes and tabulates results.

## Results

The explosive power of each device was clearly reflected by the number, size, and appearance of the pipe fragments (Fig. 1). Characterizing these features can be considered the "results" of the tests. For 2 in. × 12 in. galvanized steel, welded pipes, the number of pieces collected ranged from 4 (99% recovery) with WC-870 to 815 (87% recovery) with Winchester Action Pistol. Table 1 shows the test matrix, the percent recovery for each pipe bomb, and the total number of pieces recovered. An attempt was made to categorize the pieces as from the pipe or the end cap. Although pieces were individually weighed, only the total weight of the recovered pieces is shown in the Table. While percent recovery ranged from 51 to 99%, it averaged 87%. In the first 15 tests using a sieve only, percent recovery was less than later tests where a magnet was also used in the collection procedure.

We investigated a number of ways to characterize the power of the improvised explosive device (IED). Figures 1–3 show photos of the pipe fragments produced by Red Dot, black powder, and Bullseye powders. It is obvious that more powerful fillers, such as Red Dot and Bullseye, produced a larger number of pieces and smaller size pieces than the less powerful fillers, such as black powder. Although visual observation of the fragments clearly showed the difference in power, we looked for a simple numerical way to quantify the IED blast. To produce one numerical evaluator we considered the number of fragments from the energetic filler as a percentage of the number of fragments produced by the high explosive, nitromethane (column "exp/nm," Table 1) in the same size pipe:

$$\text{total fragments (pipe \#}5_{\text{black powder}}/\text{pipe } 13_{CH_3NO_2}) \times 100 = 9/266 = 3\%$$

Where we did not shoot nitromethane in the pipe size of interest, we used the closest pipe size, i.e., comparing a 2.5 in. diameter IMR pipe to a 2 in. diameter nitromethane pipe. This gave artifi-

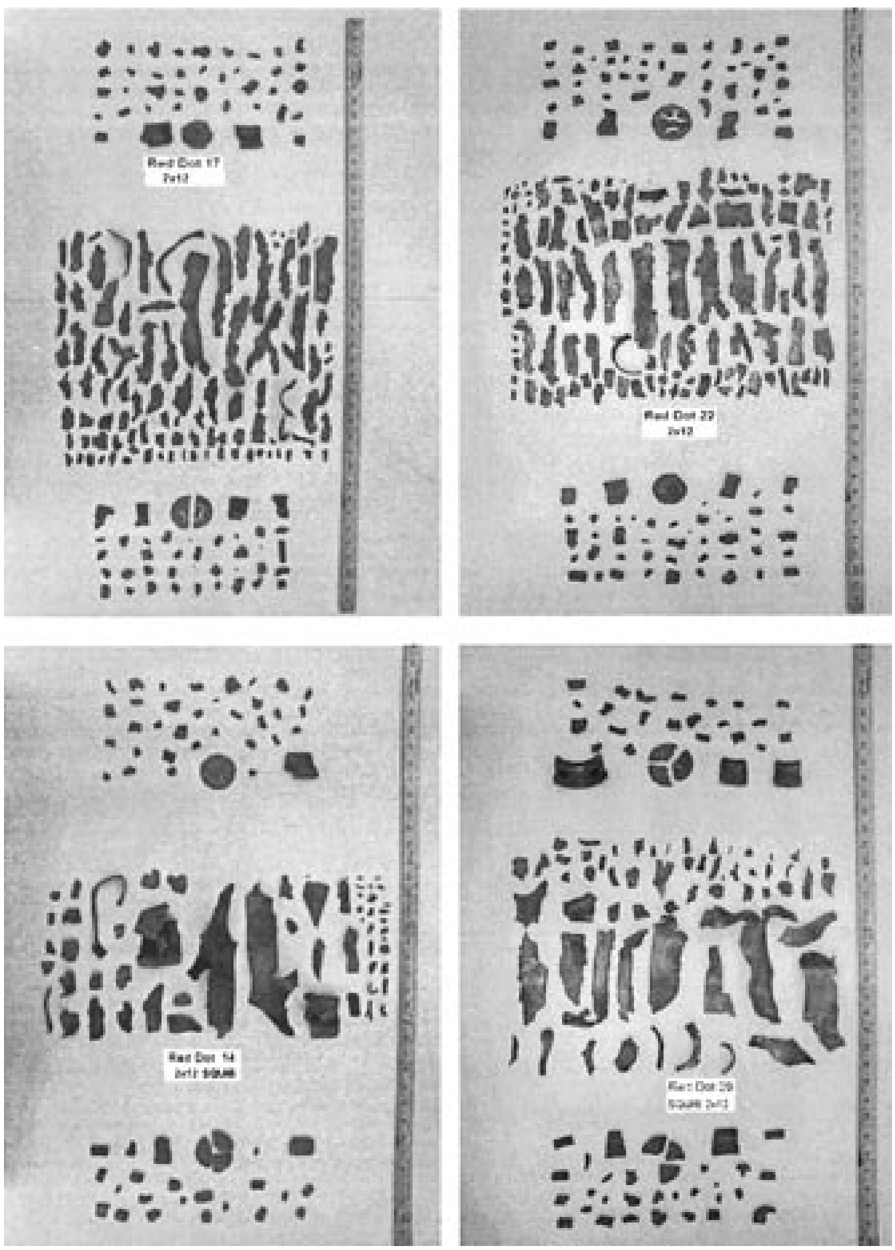

FIG. 1—*Fragments of welded steel pipes (2 in. × 12 in.) filled with Red Dot (top with detonator; bottom with squib).*

TABLE 1—*Pipe bomb observations.*

| Pipe # | Type of Pipe | Pipe Size (inches) | Orientation/ Initiator | Squib/ Detonator | Filler | Fraction Filled | Filler Weight (g) | Pipe Weight (g) | Fragment Weight (g) | Density | % Recovery | Number Fragments | | | Explosive Evaluators Percent | | |
|---|---|---|---|---|---|---|---|---|---|---|---|---|---|---|---|---|---|
| | | | | | | | | | | | | total | pipe | cap | exp/mm | frag/wt | FWDM Slope |
| 3 | steel weld | 1x6 | u/u | D | Black powder | Full | 90 | 657 | 644 | 1.17 | 98 | 7 | 5 | 2 | 7 | 8 | 0.2 |
| 38 | **PVC** | 1x6 | u/u | D | Black powder | Full | 80 | 142 | 128 | 1.04 | 90 | 370 | 368 | 2 | 349 | 462 | 13 |
| 5 | steel weld | 2x12 | u/u | D | Black powder | Full | 700 | 2514 | 2009 | 1.13 | 80 | 9 | 2 | 7 | 3 | 1 | 1.0 |
| 23 | steel weld | 2x12 | u/u | D | Black powder | Full | 689 | 2514 | 2404 | 1.12 | 96 | 22 | 12 | 10 | 8 | 3 | 2.3 |
| 9 | steel weld | 2x12 | u/u | S | Black powder | Full | 689 | 2514 | 2491 | 1.12 | 99 | 15 | 9 | 6 | 6 | 2 | 1.3 |
| 28 | steel weld | 2x12 | u/u | S | Black powder | Full | 676 | 2514 | 2378 | 1.09 | 95 | 17 | 7 | 10 | 6 | 3 | 1.2 |
| 50 | steel seamless | 2x12 | u/u | D | Black powder | Full | 676 | 2664 | 2667 | 1.09 | 100 | 20 | 2 | 18 | 8 | 3 | 2.0 |
| 1 | steel weld | 1x6 | u/u | D | WC870 | Full | 90 | 657 | 652 | 1.17 | 99 | 11 | 9 | 2 | 10 | 12 | 1.6 |
| 4 | steel weld | 2x12 | u/u | D | WC870 | Full | 662 | 2514 | 2495 | 1.07 | 99 | 4 | 3 | 2 | 2 | 1 | 0.13 |
| 24 | steel weld | 2x12 | u/u | D | WC870 | Full | 661 | 2514 | 2459 | 1.07 | 98 | 11 | 5 | 6 | 4 | 2 | 0.31 |
| 8 | steel weld | 2x12 | u/u | S | WC870 | Full | 660 | 2514 | 2451 | 1.07 | 98 | 12 | 7 | 5 | 5 | 2 | 0.32 |
| 27 | steel weld | 2x12 | u/u | S | WC870 | Full | 660 | 2514 | 2425 | 1.07 | 96 | 15 | 13 | 2 | 6 | 2 | 1.4 |
| 16 | steel weld | 1x6 | u/u | D | IMR-PB | Full | 53 | 657 | 505 | 0.68 | 77 | 65 | 33 | 30 | 61 | 124 | 11 |
| 21 | steel weld | 1x6 | u/u | S | IMR-PB | Full | 52 | 657 | 590 | 0.67 | 90 | 66 | 28 | 34 | 62 | 128 | 6.5 |
| 26 | steel weld | 2x12 | u/u | D | IMR-PB | Full | 391 | 2514 | 2049 | 0.63 | 82 | 185 | 98 | 89 | 70 | 47 | 28 |
| 31 | steel weld | 2x12 | u/u | S | IMR-PB | Full | 391 | 2514 | 2213 | 0.63 | 88 | 133 | 71 | 67 | 50 | 34 | 7 |
| 51 | steel seamless | 2x12 | u/u | D | IMR-PB | Full | 372 | 2721 | 2488 | 0.60 | 91 | 382 | 170 | 212 | 144 | 103 | 14 |
| 36 | steel weld | 2.5x15 | u/u | D | IMR PB | Full | 675 | 4593 | 4484 | 0.56 | 98 | 344 | 214 | 130 | 129 | 51 | 36 |
| 18 | steel weld | 1x6 | u/u | D | Red Dot | Full | 45 | 657 | 574 | 0.58 | 87 | 87 | 40 | 46 | 82 | 193 | 14 |
| 19 | steel weld | 1x6 | u/u | S | Red Dot | Full | 45 | 657 | 556 | 0.58 | 85 | 56 | 19 | 39 | 53 | 124 | 5 |
| 14 | steel weld | 2x12 | u/u | S | Red Dot | Full | 331 | 2514 | 1867 | 0.54 | 74 | 119 | 58 | 62 | 45 | 36 | 8.2 |
| 29 | steel weld | 2x12 | u/u | S | Red Dot | Full | 320 | 2514 | 2136 | 0.52 | 85 | 119 | 61 | 59 | 45 | 37 | 9.6 |
| 15 | steel weld | 2x12 | u/u | D | Red Dot | Full | 320 | 2514 | 1800 | 0.52 | 72 | 118 | 54 | 63 | 44 | 37 | 13 |
| 17 | steel weld | 2x12 | u/u | D | Red Dot | Full | 331 | 2514 | 2056 | 0.54 | 82 | 191 | 99 | 74 | 72 | 58 | 27 |
| 22 | steel weld | 2x12 | u/u | D | Red Dot | Full | 320 | 2514 | 2161 | 0.52 | 86 | 210 | 125 | 92 | 79 | 66 | 27 |

| | | | | | | | | | | | | | | | | | |
|---|---|---|---|---|---|---|---|---|---|---|---|---|---|---|---|---|---|
| 46 | steel weld | 2x12 | u/u | D | Red Dot | 1/2 | 160 | 2664 | 2549 | | 96 | 257 | 122 | 135 | 97 | 161 | 13 |
| 54 | steel weld | 2x12 | s/u | D | Red Dot | 1/8 | 46 | 2343 | 2321 | | 99 | 6 | 1 | 5 | 2 | 13 | 0.8 |
| 55 | steel weld | 2x12 | s/u | D | Red Dot | 1/4 | 91 | 2429 | 2369 | | 98 | 157 | 9 | 148 | 59 | 171 | 10 |
| 53 | steel weld | 2x12 | s/u | D | Red Dot | 1/2 | 183 | 2343 | 2252 | | 96 | 415 | 87 | 328 | 156 | 227 | 8.0 |
| 45 | steel weld | 2x12 | s/u | D | Red Dot | 1/2 | 160 | 2551 | 2371 | | 93 | 18 | 6 | 12 | 7 | 11 | 2.6 |
| 47 | steel weld | 2x12 | s/u | D | Red Dot | 3/4 | 240 | 2608 | 2331 | | 89 | 299 | 85 | 214 | 112 | 125 | 13 |
| 48 | steel weld | 2x12 | s/u | D | Red Dot | Full | 320 | 2296 | 2269 | 0.52 | 99 | 710 | 110 | 600 | 267 | 222 | 15 |
| 34 | steel weld | 2.5x15 | u/u | D | Red Dot | Full | 600 | 4593 | 4346 | 0.50 | 95 | 286 | 165 | 120 | 108 | 48 | 23 |
| 35 | steel weld | 2.5x15 | u/u | S | Red Dot | Full | 600 | 4593 | 4483 | 0.50 | 98 | 238 | 121 | 118 | 89 | 40 | 6 |
| 2 | steel weld | 1x6 | u/u | D | Bullseye | Full | 58 | 657 | 559 | 0.74 | 85 | 124 | 61 | 60 | 117 | 216 | 26 |
| 11 | steel weld | 1x6 | u/u | S | Bullseye | Full | 61 | 657 | 565 | 0.79 | 86 | 53 | 18 | 35 | 50 | 87 | 2.8 |
| 20 | steel weld | 1x6 | u/u | S | Bullseye | Full | 58 | 657 | 612 | 0.75 | 93 | 72 | 26 | 46 | 68 | 12 | 3.2 |
| 39 | **PVC** | 1x6 | u/u | D | Bullseye | Full | 50 | 142 | 103 | 0.65 | 73 | 380 | 376 | 1 | 358 | 760 | 4.2 |
| 40 | steel weld | 1.5x12 | u/u | D | Bullseye | 1/2 | 145 | 1701 | 1593 | | 94 | 558 | 168 | 390 | 210 | 385 | 47 |
| 41 | steel weld | 1.5x12 | s/u | D | Bullseye | 1/2 | 145 | 1701 | 1561 | | 92 | 701 | 205 | 496 | 264 | 483 | 15 |
| 52 | steel weld | 1.5x12 | s/u | D | Bullseye | 3/4 | 217 | 1729 | 1666 | | 96 | 623 | 158 | 473 | 234 | 287 | 15 |
| 56 | steel weld | 1.5x12 | s/u | D | Bullseye | Full | 257 | 1714 | 1493 | | 87 | 614 | 149 | 465 | 231 | 239 | 27 |
| 6 | steel weld | 2x12 | u/u | D | Bullseye | Full | 420 | 2514 | 1646 | 0.68 | 65 | 221 | 134 | 87 | 83 | 53 | 31 |
| 25 | steel weld | 2x12 | u/u | D | Bullseye | Full | 437 | 2514 | 1854 | 0.71 | 74 | 258 | 166 | 91 | 97 | 59 | 45 |
| 10 | steel weld | 2x12 | u/u | S | Bullseye | Full | 437 | 2514 | 1901 | 0.71 | 76 | 122 | 86 | 36 | 46 | 28 | 8 |
| 30 | steel weld | 2x12 | u/u | S | Bullseye | Full | 437 | 2514 | 2160 | 0.71 | 86 | 145 | 78 | 67 | 55 | 33 | 4.6 |
| 49 | steel seamless | 2x12 | u/u | D | Bullseye | Full | 405 | 2714 | 2461 | 0.66 | 91 | 447 | 235 | 212 | 168 | 110 | 34 |
| 32 | steel weld | 2.5x15 | u/u | S | Bullseye | Full | 795 | 4593 | 3297 | 0.66 | 72 | 148 | 94 | 54 | 56 | 19 | 14 |
| 33 | steel weld | 2.5x15 | u/u | D | Bullseye | Full | 800 | 4593 | 3222 | 0.66 | 70 | 310 | 194 | 116 | 117 | 39 | 37 |
| 42 | steel weld | 1x6 | u/u | D | Winchester A.P. | Full | 48 | 624 | 529 | 0.62 | 85 | 630 | 163 | 467 | 594 | 1313 | 56 |
| 44 | steel weld | 2x12 | u/u | D | Winchester A.P. | Full | 550 | 2664 | 2307 | 0.89 | 87 | 815 | 533 | 282 | 306 | 148 | 56 |
| 43 | steel weld | 1.5x12 | u/u | D | $NaClO_3$/Al | Full | 539 | 1786 | 1639 | 1.55 | 92 | 647 | 146 | 501 | 243 | 120 | 28 |
| 12 | steel weld | 1x6 | u/u | D | $MeNO_2$ | Full | 82 | 657 | 407 | 1.06 | 62 | 106 | 67 | 39 | 100 | 129 | 24 |
| 13 | steel weld | 2x12 | u/u | D | $MeNO_2$ | Full | 732 | 2514 | 1283 | 1.18 | 51 | 266 | 158 | 108 | 100 | 36 | 35 |
| 37 | steel weld | 1.5x12 | u/u | D | Grit-o-Cob ® | | blank | | | 7 | steel weld | | 1x6 | up/up | D | | |

Pipes 1-37 shot in sand; pipes 38-52 shot in Grit-o-Cob ®

* u/u = vertical, initiator in end; s/u = horizontal pipe, initiator in end

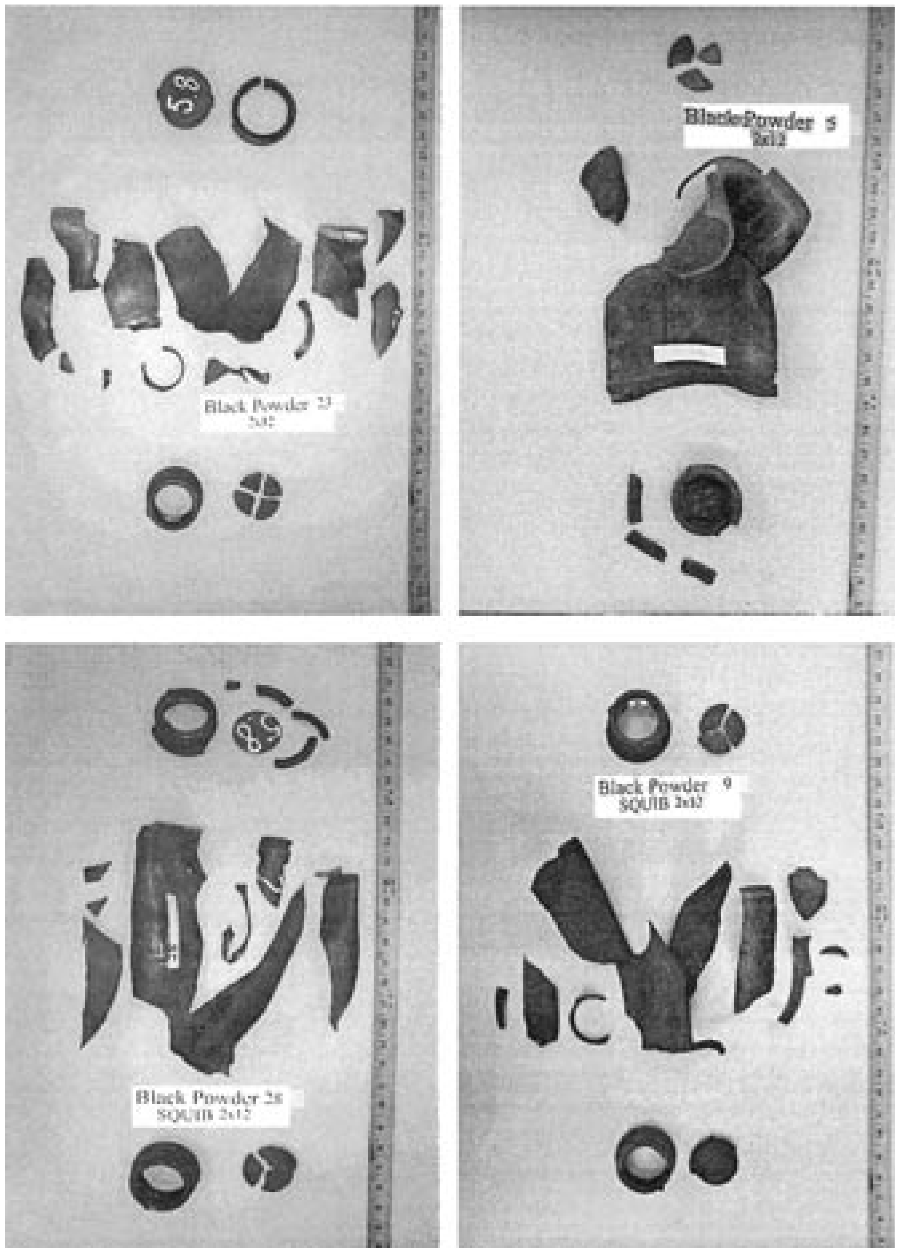


FIG. 2—*Fragments of welded steel pipes (2 in. × 12 in.) filled with black powder (top with detonator; bottom with squib).*

cially high values. For this reason, we found the "exp/nm" evaluator was not as useful as others, since to avoid values greater than 100% we should have shot nitromethane calibrations under identical conditions as the pipe bomb being evaluated. We created a second numerical evaluator by dividing the number of fragments produced by a bomb by the weight of its energetic filler (column "frag/wt"). The number is multiplied by 100 and expressed as "%" to make it nonfractional.

$$\text{(total fragments pipe \#5/weight of black powder \#5)} \times 100 = 9/700 = 1\%$$

However, the magnitude of the "frag/wt" evaluator appeared dependent on the device size. Furthermore, both evaluators would be distorted if fragment recoveries were less than 100%, a difficult requirement at a real incident scene. Therefore, we looked for a third evaluator which would allow us to rate the violence of an event from partial fragment recovery.

The third numerical evaluator, which we termed "Fragment Weight Distribution Mapping" (FWDM), (3,4) accounts for fragment number and size without requiring complete recovery. This evaluator compensates for the fact that total pipe weight or recovery of pipe will vary from pipe to pipe by using a percentage of fragment weight over total recovered pipe weight instead of using absolute fragment weight directly. The abscissa ($x$) is the weight of a single fragment ($m_x$) divided by the total weight of all recovered fragments ($M_r$). (The calculation can be simplified by using the weight of all fragments in a given weight category as the numerator. This will greatly accelerate the calculation, especially if it is applied to a large number of tiny fragments.) The ordinate ($y$) reflects how much of the

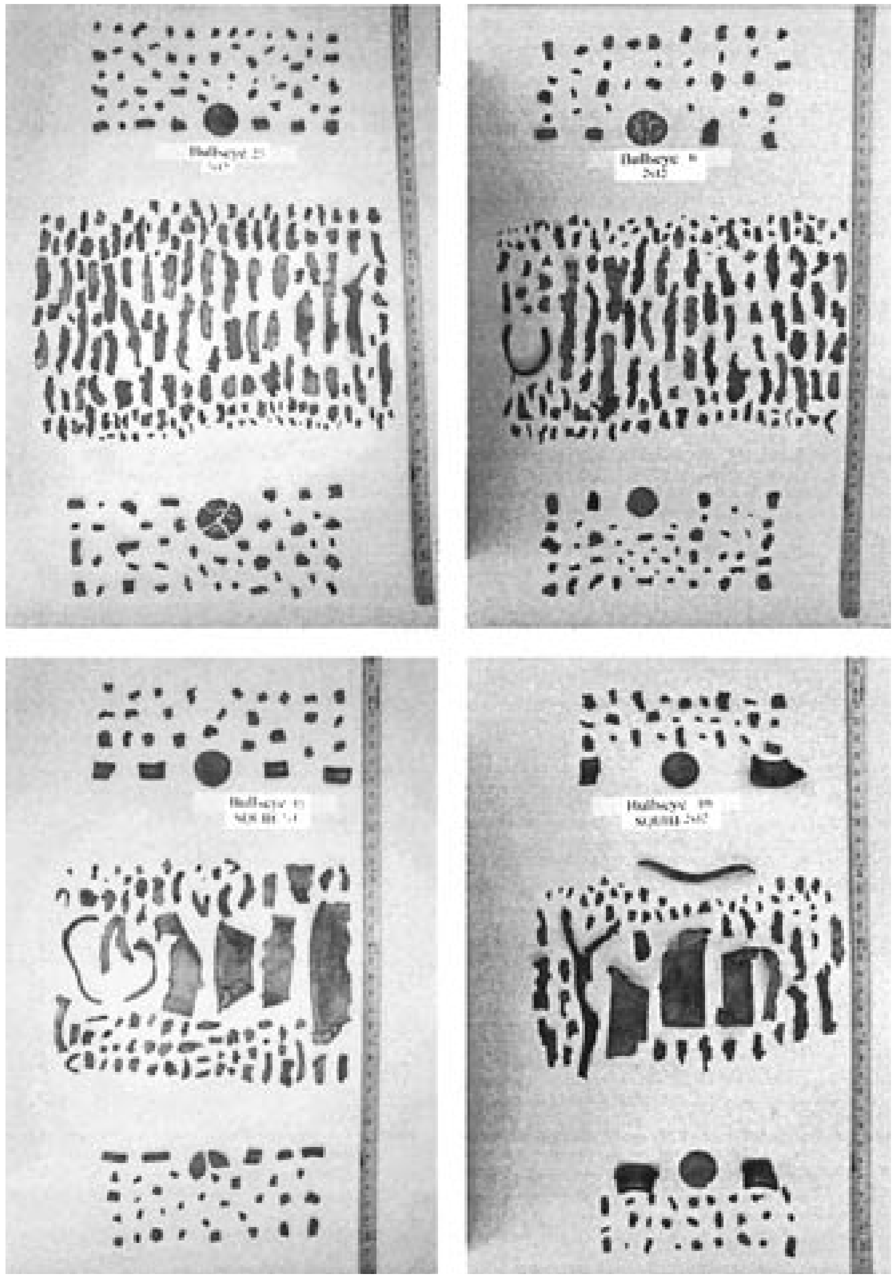

FIG. 3—*Fragments of welded steel (2 in. × 12 in.) pipes filled with Bullseye (top with detonator; bottom with squib).*

pipe is accounted for by the largest pieces. It uses the sum of the single fragment weight (or total weight in a category) with all fragments larger than it [sum $(m_1 + m_2 + m_3 \ldots + m_x)$]. This value is also divided by the total recovered weight ($M_r$) to normalize it. Furthermore, the logarithm of this value is used, so that the ordinate becomes log {[100 × (weight of all heavier fragments)]/(total weight of all fragments)} or log {[sum $(m_1 + m_2 + m_3 \ldots + m_x)$]/$(M_r)$}. Using logarithms tends to play down minor variations and accentuate major variations. Dividing both the individual fragment weight (*x* axis) and the sum of all fragments as large or larger (*y* axis) by the total recovered fragment weight means that plots can be used to compare pipes of unequal weight, size, or collection efficiencies!

FWDM were found to be reproducible and relatively insensitive to percentage recovery (Figs. 4, 5). When recovery is incomplete, it tends to be the small fragments that are lost. Since small fragments end up being plotted near the origin of the graph, they do not have the effect on the slope that larger fragments do. The larger fragments tend to dictate the slope, and it is the slope of the FWDM plots that differentiates the magnitude of the blast. High or medium-energy events, which produced many small fragments, were recognizable by steep slopes, while low-energy events, which formed few fragments, plotted shallow slopes. The outcome of the FWDM can be expressed in a single variable—the slope of the plot (Column "FWDM slope" Table 1). Figures 6 and 7 shows the FWDM plots for the test results previously shown in Figs. 2 and 3.

The visual differentiation between low- and high-energy events is reflected succinctly in the numerical evaluators. The low-energy fillers, black powder and WC870, produced only 3 to 6% of the number of fragments produced by nitromethane (Table 1, column "exp/nm"); only 0.01 to 0.02 fragments per gram filler weight (Table

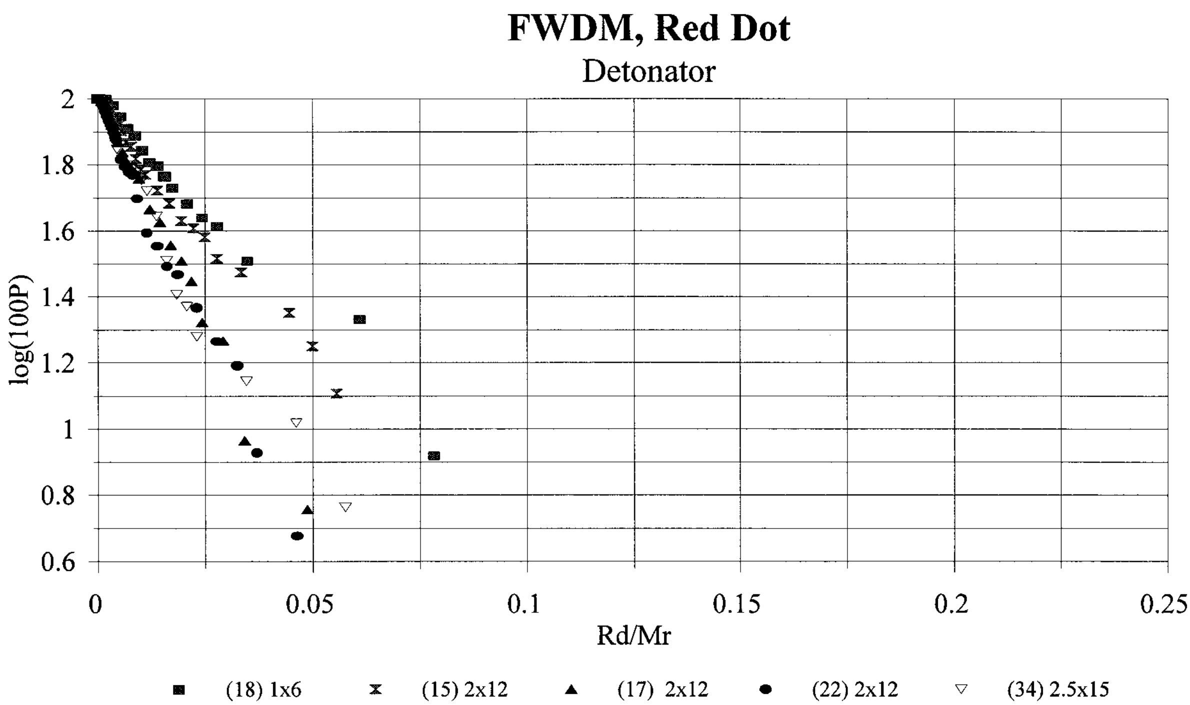


FIG. 4—*FWDM showing effect of pipe size for Red Dot in steel pipe initiated by detonator.*

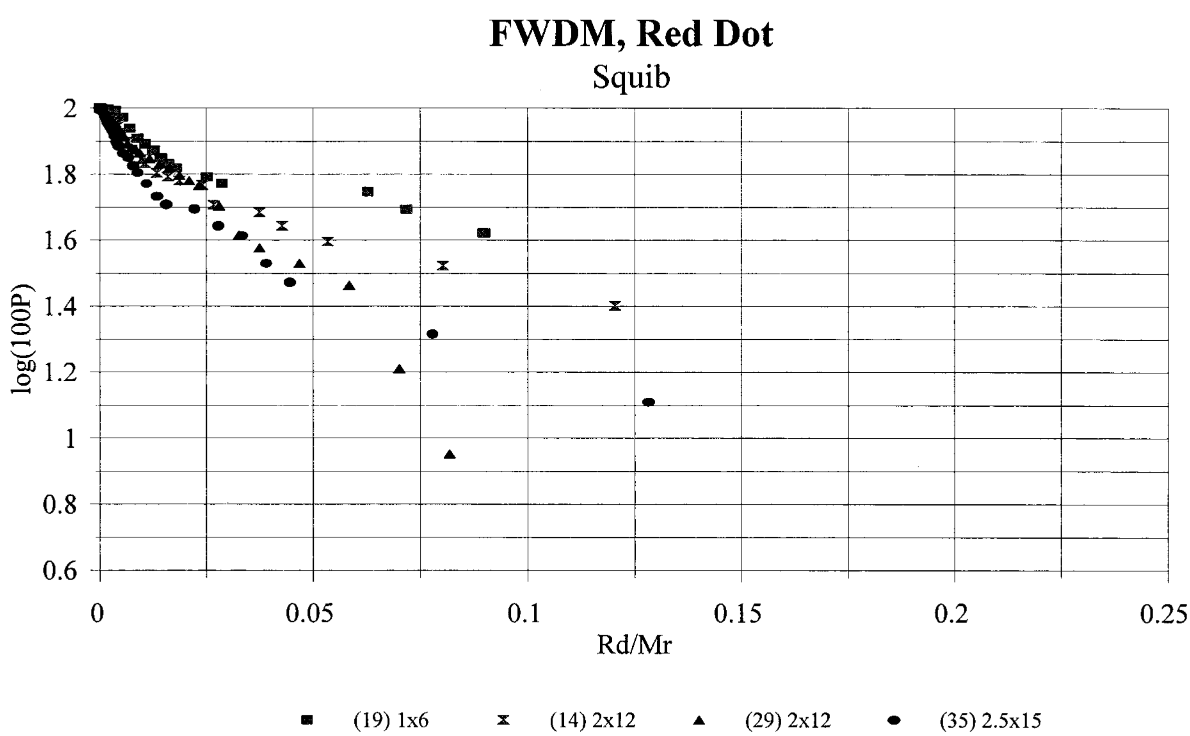


FIG. 5—*FWDM showing effect of pipe size with Red Dot in steel pipe initiated by squib.*

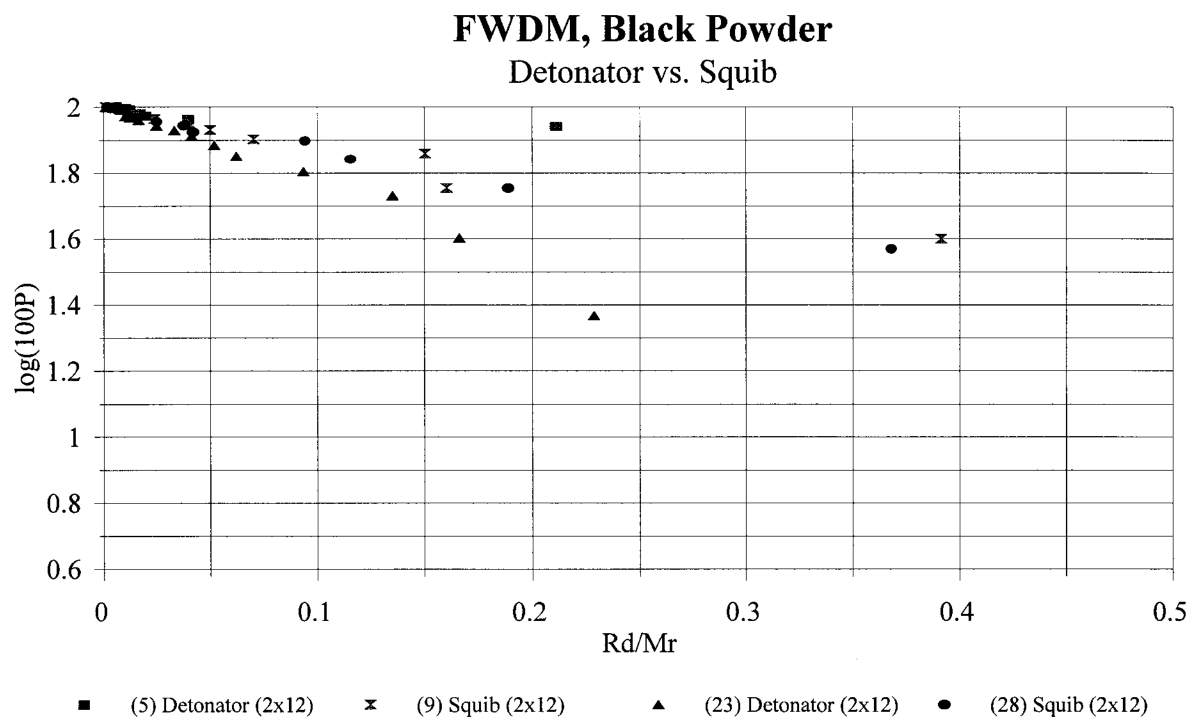


FIG. 6—*FWDM of fragments shown in photo 2 (black powder).*

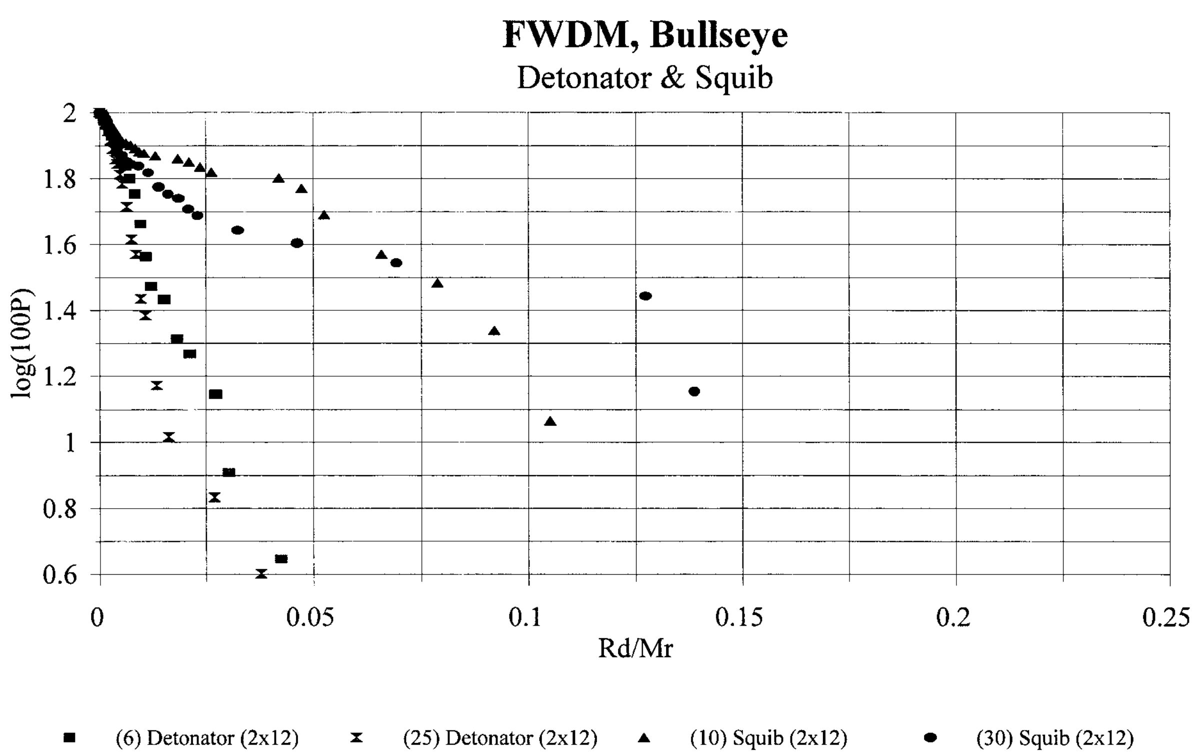


FIG. 7—*FWDM of fragments shown in photo 3 (Bullseye).*

1, column "frag/wt"), and a shallow FWDM slope (0.2 to 2). For high-energy events, the evaluators ranged from 65 to 90% (exp/nm), from 31 to 56% (exp/wt), and from 22 to 56 (FWDM), for comparison with nitromethane fragmentation (column "exp/nm"), fragments versus weight (column "frag/wt") (Table 2, detonator initiation).

Having determined several ways to simply describe the results of a pipe bomb explosion, we addressed essential issues concerning the characteristics of these explosions.

### *Reproducibility of Fragmentation Under Identical Explosion Condition*

The photos in Figs. 1–3 show the pipe bomb fragments from 2 in. × 12 in. pipes containing Red Dot, black powder, and Bullseye, respectively. These illustrate the marked degree of reproducibility in fragments for identically prepared devices. They also indicate the vast difference in response between a lower energy material like black powder and a high-energy material like Bullseye. Reproducibility is also evident in the FWDM plots, e.g., Red Dot (Fig. 4).

### *Effects of the Initiator (Squib vs. Detonator) on Fragmentation*

From the photos showing the pipe bomb fragments from 2 in. × 12 in. pipes containing black powder (Fig. 2), Red Dot (Fig. 1), and Bullseye (Fig. 3), it is clear that Red Dot and Bullseye underwent substantially less complete reactions when a squib rather than a detonator was used. In contrast, the results with black powder appeared similar with the squib and the detonator. The same trend can also be observed by examining FWDMs. The FWDMs of powerful fillers such as Bullseye (Fig. 7), IMR-PB (Fig. 8), or Red Dot (Fig. 9) show consistently shallower slopes for squib initiation versus detonator (see Table 2). The FWDM for the less powerful

TABLE 2—*Average of numerical evaluators.**

| | | Detonator Initiation | | | | Squib Initiation | | | |
|---|---|---|---|---|---|---|---|---|---|
| | Density | # Pipes | exp/nm | frag/wt | FWDM Slope | # Pipes | exp/nm | frag/wt | FWDM Slope |
| WC-870 | 1.1 | 2 | 2.8% | 1.1% | 0.22 | 2 | 5.1% | 2.0% | 0.86 |
| Black powder | 1.1 | 2 | 5.8% | 2.2% | 1.7 | 2 | 6.0% | 2.3% | 1.25 |
| Red Dot | 0.53 | 3 | 65% | 53% | 22 | 2 | 45% | 37% | 9 |
| IMR-PB | 0.63 | 1 | 70% | 47% | 28 | 1 | 50% | 34% | 7 |
| Bullseye | 0.71 | 2 | 90% | 56% | 38 | 2 | 50% | 31% | 6 |
| $NaClO_3$/Al | 1.6 | 1 | 243%† | 120% | 28 | | | | |
| Winchester | 0.89 | 1 | 306%‡ | 148% | 56 | | | | |
| $MeNO_2$ | 1.1 | 1 | … | 36% | 35 | | | | |

*All pipes are galvanized steel 2 in. × 12 in. welded and vertical and end initiated. †Pipe was 1.5" × 12". ‡Liquid explosive.

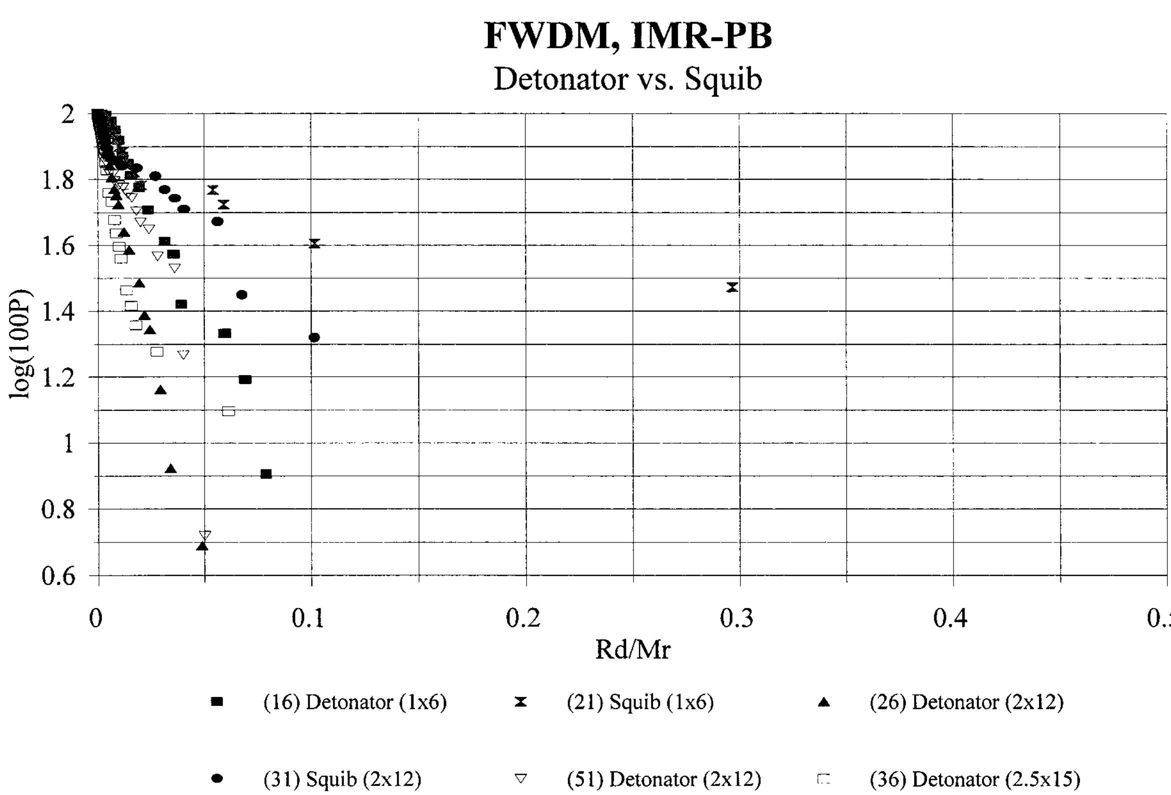


FIG. 8—*FWDM of fragments showing effects of initiator in pipes full of IMR-PB.*

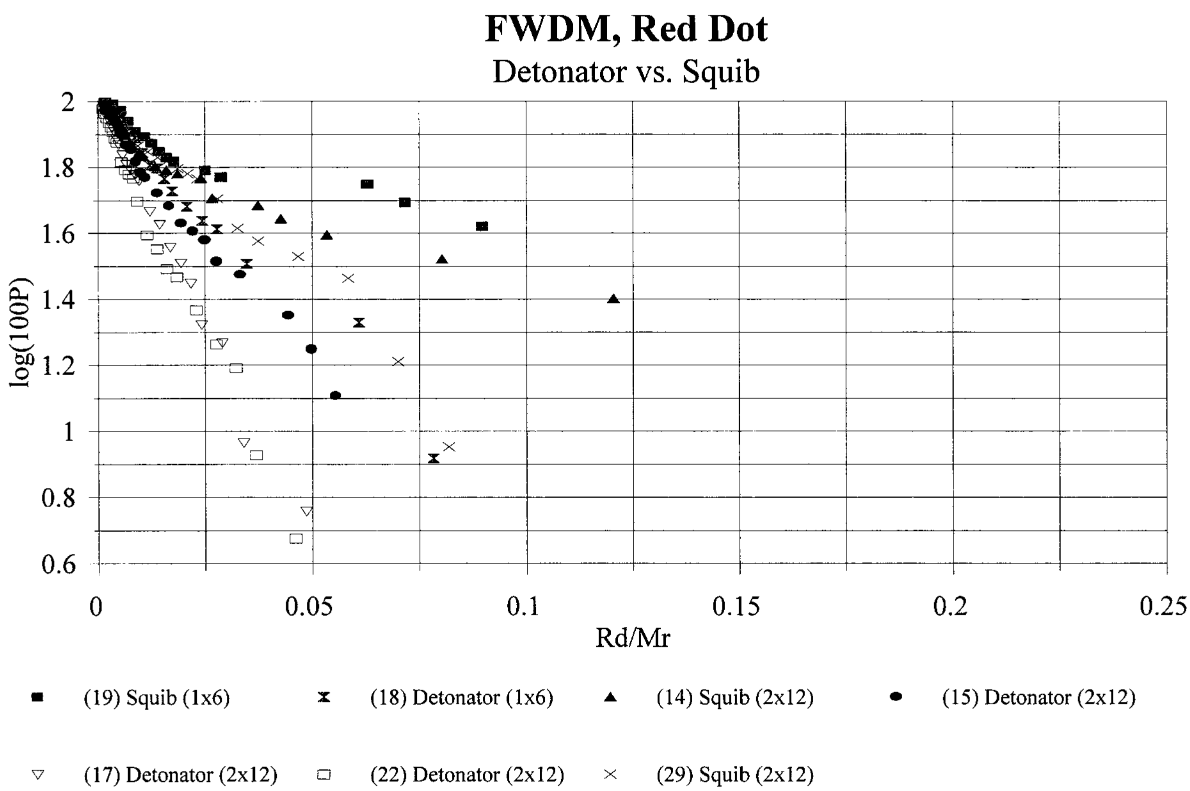


FIG. 9—*FWDM of fragments showing effects of initiator in pipes full of Red Dot.*

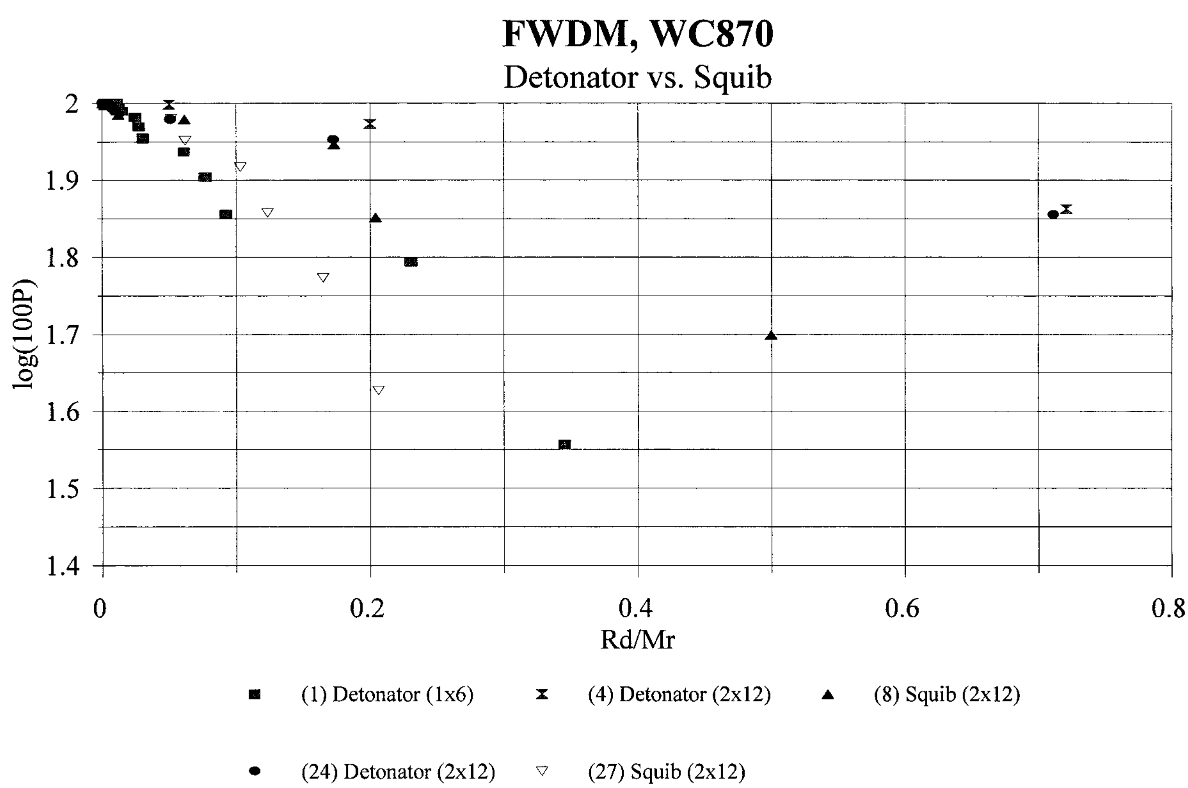


FIG. 10—*FWDM of fragments showing effects of initiator in pipes full of WC-870.*

fillers, WC-870 (Fig. 10) or black powder (Fig. 6), are somewhat scattered, but the detonator initiated material is not differentiated from the squib initiated material. The less powerful fillers, which never come close to detonation, deflagrate when initiated by flame; shock initiation can instigate no greater response. On the other hand, the higher energy materials are more likely to transit to detonation when initiated with a shock wave than an electric spark (i.e., squib).

*Effects of Pipe Size on Fragmentation*

In most tests the length to diameter (L/D) ratio was set at 6/1. Pipes ranged in size from 1 in. × 6 in. (14 pipes) and 2 in. × 12 in. (31 pipes) to 2.5 in. × 15 in. (five pipes) and 1.5 in. × 12 in. (six pipes) with energetic material weights from 0.5 to 2 lbs. As the size of the pipe and the weight of the energetic filler increased, the number of fragments formed also increased. For example, IMR-PB formed 65 pieces (77% recovery) in the 1 in. diameter pipes, 185 pieces (82% recovery) in the 2 in. diameter pipes, and 344 pieces (98% recovery) in the 2.5 in. diameter pipes (Fig. 8). However, this trend is not necessarily reflected in the slopes of the FWDMs (Table 3). For IMR-PB, the smaller diameter pipes do produce slightly shallower FWDM slopes, but for Bullseye and Red Dot this tendency is slight (Figs. 9 and 11) (see Table 3). Compared to the difference in FWDM slopes between detonator versus squib initiation, it is hardly noticeable. The independence of the FWDM from device size is considered a positive feature. The FWDM of black powder (Fig. 6) shows essentially no size effects. We speculate that the slight increase in the slope of the FWDM observed with the high-energy fillers results because at larger diameter, they come close to supporting a detonation wave. A detonation requires a certain amount of energy in the reaction front; thus, a material of too small a diameter cannot support detonation. Black powder lacks sufficient energy to detonate; therefore, diameter makes little difference in the slope of the FWDM. Photos of Bullseye devices (1″, 2″, and 2.5″) illustrate that increased size has only a slight effect on fragmentation (Fig. 12). One obvious difference is the increased fragmentation of the end caps.

*Effects of the Types of the Energetic Filler on Fragmentation*

Eight energetic fills were tested (number of replicates is indicated in parentheses): black powder (7); WC 870 (5); IMR-PB (6); Winchester Action Pistol (2); chlorate/aluminum paint (1); Red Dot (16); Bullseye (15); and nitromethane (2). Explosive power was assessed by visual observation as well as by the three numeric evaluators. Although on average the numerical evaluators showed the same trends (Table 2), we found that the FWDM slopes (Fig. 13) were more reliable in expressing the power of the filler than the total number of fragments or either of the evaluators based on number of fragments (exp/nm or frag/wt). From left (least powerful) to

TABLE 3—*Effect of pipe size on fragmentation.*

| Detonator Initiated | | | Fragments | | Percent | | FWDM | Squib Initiated | | Fragments | | Percent | | FWDM |
|---|---|---|---|---|---|---|---|---|---|---|---|---|---|---|
| # | In. | Fill Type | % | Total # | exp/nm | frag/wt | Slope | # | In. | % | Total # | exp/nm | frag/wt | Slope |
| 3 | 1 × 6 | Black powder | 98 | 7 | 7 | 8 | 0.2 | | | | | | | |
| 5 | 2 × 12 | " | 80 | 9 | 8 | 1 | 1.0 | 9 | 2 × 12 | 99 | 15 | 14 | 2 | 1.3 |
| 23 | " | " | 96 | 22 | 21 | 3 | 2.3 | 28 | " | 95 | 17 | 16 | 3 | 1.2 |
| 1 | 1 × 6 | WC870 | 99 | 11 | 10 | 12 | 1.6 | | | | | | | |
| 4 | 2 × 12 | " | 99 | 4 | 4 | 1 | 0.1 | 8 | 2 × 12 | 98 | 12 | 11 | 2 | 0.3 |
| 24 | " | " | 98 | 11 | 10 | 2 | 0.3 | 27 | " | 96 | 15 | 14 | 2 | 1.4 |
| 16 | 1 × 6 | IMR-PB | 77 | 65 | 61 | 124 | 11 | 21 | 1 × 6 | 90 | 66 | 62 | 128 | 7 |
| 26 | 2 × 12 | " | 82 | 185 | 175 | 47 | 28 | 31 | 2 × 12 | 88 | 133 | 125 | 34 | 7 |
| 36 | 2.5 × 15 | " | 98 | 344 | 325 | 51 | 36 | | | | | | | |
| 18 | 1 × 6 | Red Dot | 87 | 87 | 82 | 193 | 14 | 19 | 1 × 6 | 85 | 56 | 53 | 124 | 5 |
| 15 | 2 × 12 | " | 72 | 118 | 111 | 37 | 13 | 14 | 2 × 12 | 74 | 119 | 112 | 36 | 8 |
| 17 | " | " | 82 | 191 | 180 | 58 | 27 | 29 | " | 85 | 119 | 112 | 37 | 10 |
| 22 | " | " | 86 | 210 | 198 | 66 | 27 | | | | | | | |
| 34 | 2.5 × 15 | " | 95 | 286 | 270 | 48 | 23 | 35 | 2.5 × 15 | 98 | 238 | 225 | 40 | 6 |
| 2 | 1 × 6 | Bullseye | 85 | 124 | 117 | 216 | 26 | 11 | 1 × 6 | 86 | 53 | 50 | 87 | 3 |
| | | | | | | | | 20 | 1 × 6 | 93 | 72 | 68 | 124 | 3 |
| 6 | 2 × 12 | " | 65 | 221 | 208 | 53 | 31 | 10 | 2 × 12 | 76 | 122 | 115 | 28 | 8 |
| 25 | " | " | 74 | 258 | 243 | 59 | 45 | 30 | " | 86 | 145 | 137 | 33 | 5 |
| 33 | 2.5 × 15 | " | 70 | 310 | 292 | 39 | 37 | 32 | 2.5 × 15 | 72 | 148 | 140 | 19 | 14 |
| 42 | 1 × 6 | Winchester A.P. | 85 | 630 | 594 | 1313 | 56 | | | | | | | |
| 44 | 2 × 12 | " | 87 | 815 | 769 | 148 | 56 | | | | | | | |
| 43 | 1.5 × 12 | $NaClO_3$/Al | 92 | 647 | 610 | 120 | 28 | | | | | | | |
| 12 | 1 × 6 | $MeNO_2$ | 62 | 106 | 100 | 129 | 24 | | | | | | | |
| 13 | 2 × 12 | " | 51 | 266 | 251 | 36 | 35 | | | | | | | |

Pipes are galvanized, welded steel shot vertically with initiation in one end.

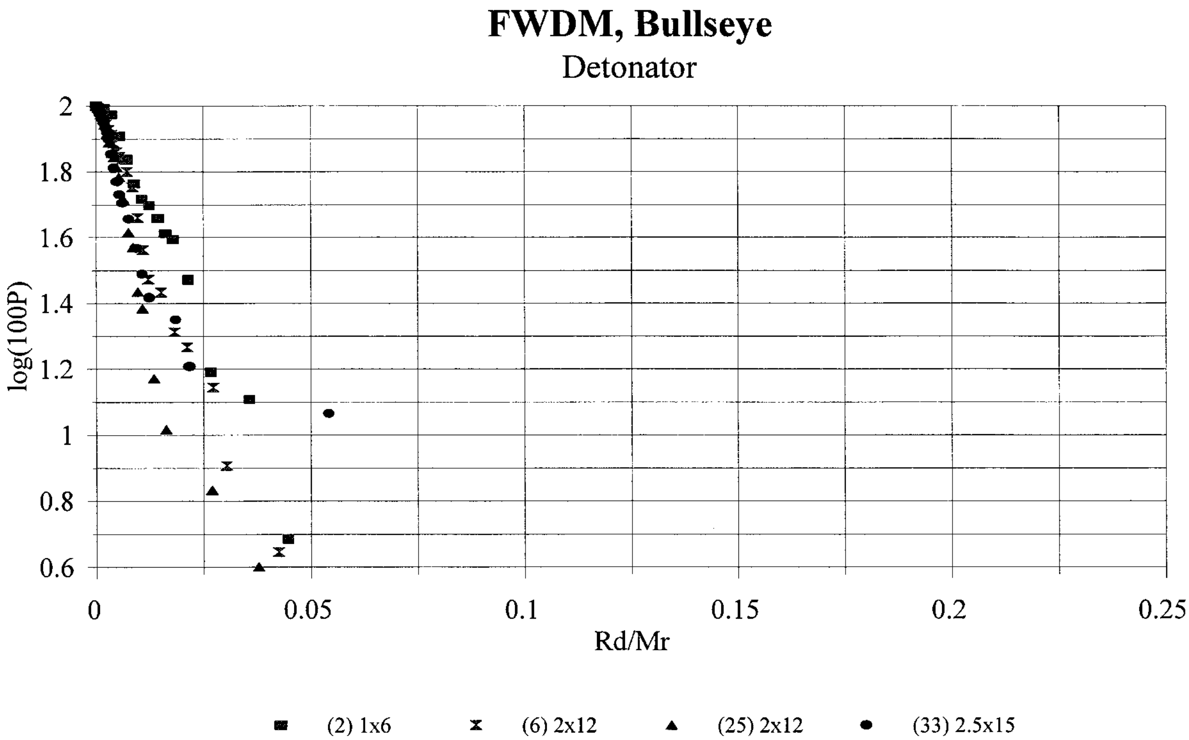


FIG. 11—*FWDM showing effect of pipe size for Bullseye in steel pipe initiated by detonator.*

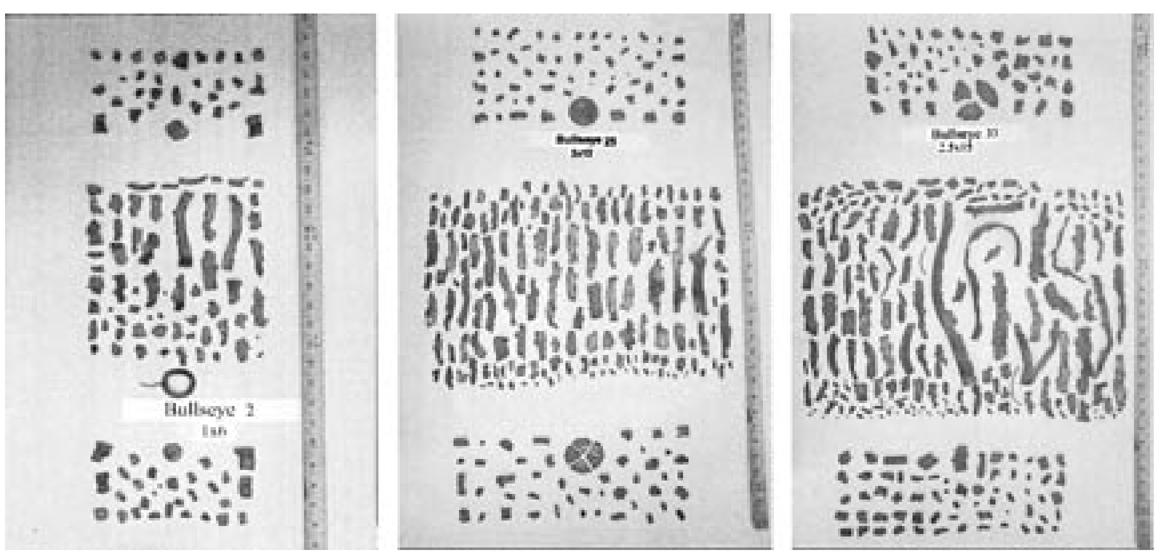


FIG. 12—*Fragments of Welded Steel Pipes (from left to right, 1 in., 2 in. or 2.5 in. diameter) filled with Bullseye.*

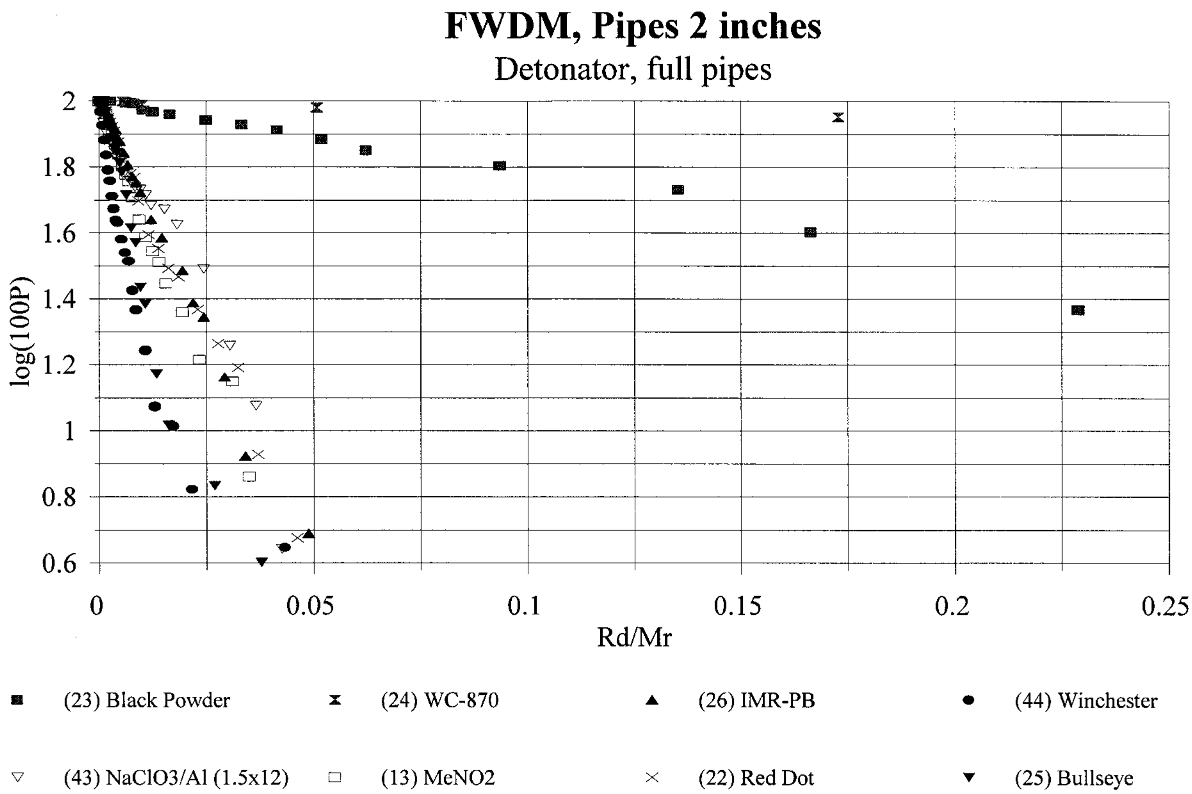


FIG. 13—*FWDM comparing all fillers in 2 in. × 12 in. welded steel pipes with detonator initiation.*

right (most powerful) all three numeric evaluators give the same basic order:

WC-870 ~ black powder < Red Dot

~ IMR < Bullseye < Winchester A.P.

Although the evidence strongly supports this order, we are somewhat surprised that Winchester Action Pistol (A.P.), rather than Bullseye, appeared to be the most powerful. One reason for this difference may be the change in our test protocol from using sand to stop the fragments (pipes 1–37) to using Grit-o-Cob® to stop them (pipes 38–56). Pipes shot in the latter mixture, which include the two pipes containing Winchester A.P. powder, appeared to produce somewhat more fragmentation than those shot in the former. This confinement effect will be addressed in future studies.

*Effects of Pipe Material on Fragmentation*

Most (51) pipes were schedule 40, galvanized, steel, butt-end welded, but a few pipe bombs were cased in seamless steel (3) or PVC (2). When seamless steel pipes were used with IMR-PB or Bullseye filler, the number of pipe fragments increased twofold; for black powder there was essentially no change (Table 4). How-

TABLE 4—*Effect of pipe material on fragmentation.*

| # | Pipe Material | Dim. (in) | % | # Fragments Total | Pipe | Cap | Evaluators exp/nm% | frag/wt% | FWDM Slope |
|---|---|---|---|---|---|---|---|---|---|
| | | | | Black Powder (1.1 g/cc) | | | | | |
| 3 | gal. steel weld | 1 × 6 | 98 | 7 | 5 | 2 | 7 | 8 | 0.2 |
| 38 | PVC | 1 × 6 | 90 | 370 | 368 | 2 | 349 | 462 | 13 |
| 5 | gal. steel weld | 2 × 12 | 80 | 9 | 2 | 7 | 8 | 1 | 1 |
| 23 | gal. steel weld | 2 × 12 | 96 | 22 | 12 | 10 | 21 | 3 | 2 |
| 50 | seamless steel | 2 × 12 | 100 | 20 | 2 | 18 | 19 | 3 | 2 |
| | | | | IMR-RP (0.63 g/cc) | | | | | |
| 26 | gal. steel weld | 2 × 12 | 82 | 185 | 98 | 89 | 175 | 47 | 28 |
| 51 | seamless steel | 2 × 12 | 91 | 382 | 170 | 212 | 360 | 103 | 14 |
| | | | | Bullseye (0.70 g/cc) | | | | | |
| 2 | gal. steel weld | 1 × 6 | 85 | 124 | 61 | 60 | 117 | 216 | 26 |
| 39 | PVC | 1 × 6 | 73 | 380 | 376 | 1 | 358 | 760 | 4 |
| 6 | gal. steel weld | 2 × 12 | 65 | 221 | 134 | 87 | 208 | 53 | 31 |
| 25 | gal. steel weld | 2 × 12 | 74 | 258 | 166 | 91 | 243 | 59 | 45 |
| 49 | seamless steel | 2 × 12 | 91 | 447 | 235 | 212 | 422 | 110 | 34 |

Detonators were used to initiate these vertical pipes at one end.

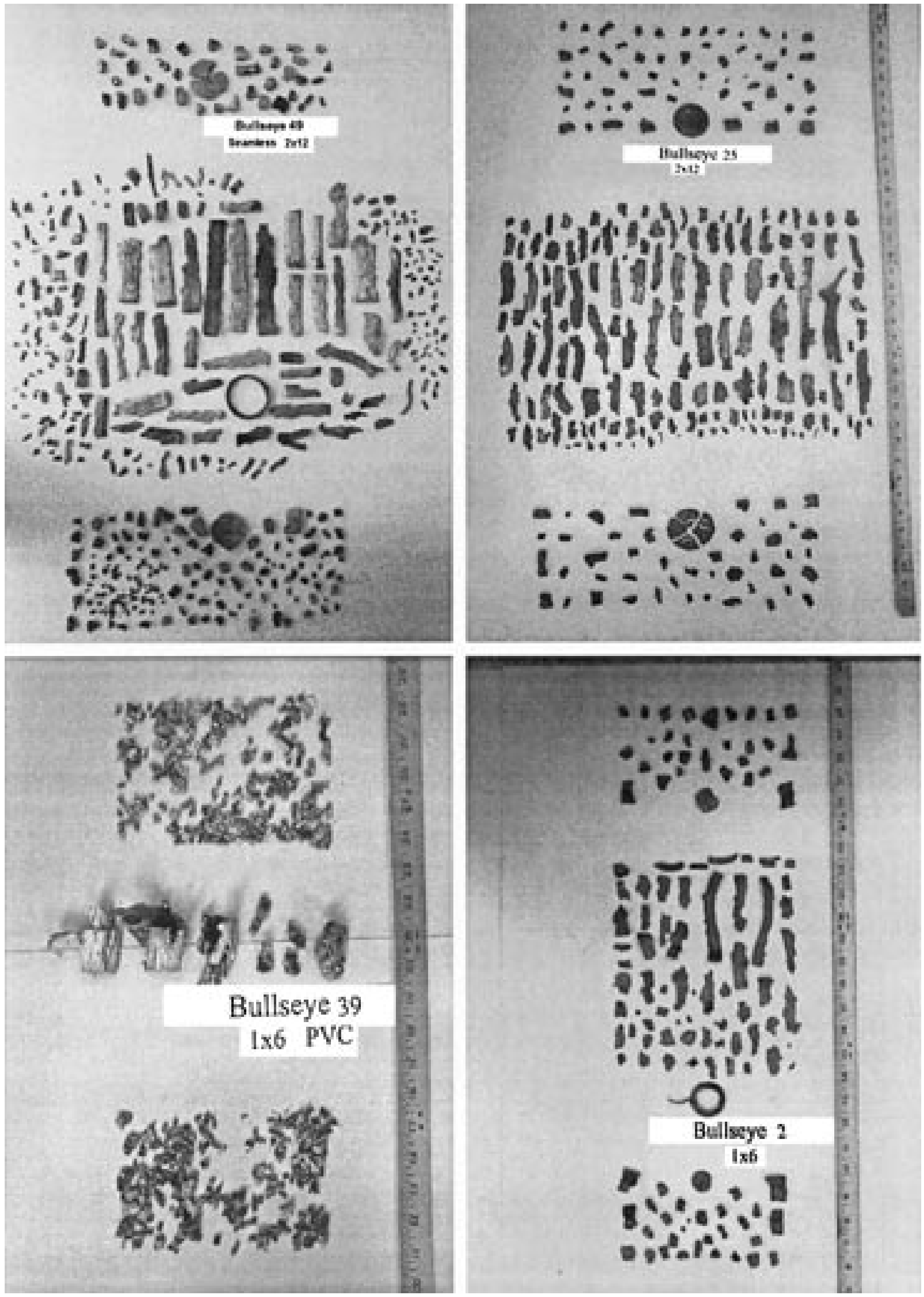


FIG. 14—*Fragments of pipes filled with Bullseye (left to right: top—seamless steel, seamed steel, 2" × 12"; bottom—PVC, seam steel, 1" × 6").*

ever, in this case the number of fragments does not accurately convey the fragmentation picture, and even the FWDM plots are somewhat confusing since the slope of the seamless plot starts out steeper and ends up shallower than that of the seamed pipes. Figures 14–17 are photos of the pipe fragments and the FWDM plots for Bullseye and IMR-PB, respectively. In both cases, the seamless 2 in. × 12 in. pipe produced more fragments than the seamed pipe, but the fragments arise primarily from the end caps of the pipes. Most of the pieces from the main body of the pipe are actually larger for the seamless pipe than for the seamed one. This phenomena is not observed with black powder. Figures 18 and 19 show little difference in the fragmentation of the seamed and seamless.

We believe that the fragmentation of the pipe depends in part on the relationship between the deflagration rate of the filler and the speed of sound in the pipe walls. High-energy materials, such as Bullseye and IMR-PB, deflagrate so quickly that high pressure throughout the pipe is achieved instantly, and failure occurs at

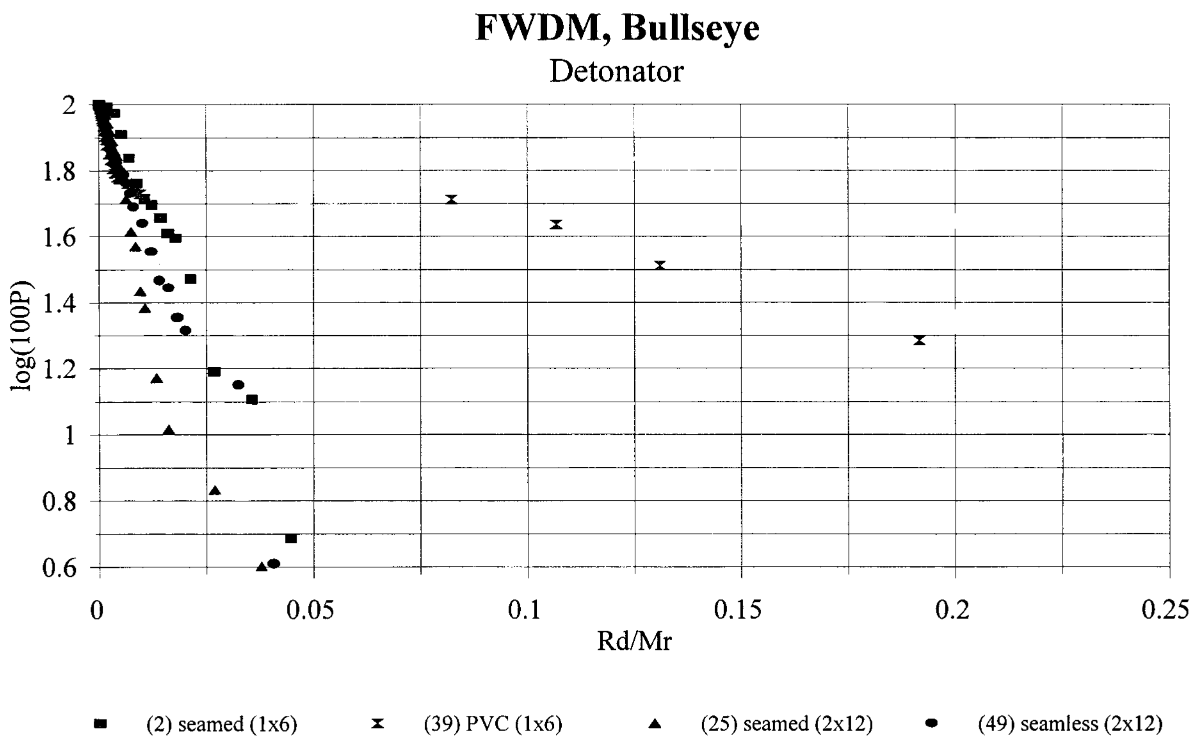


FIG. 15—*FWDM of fragments shown in Photo 14 (Bullseye).*

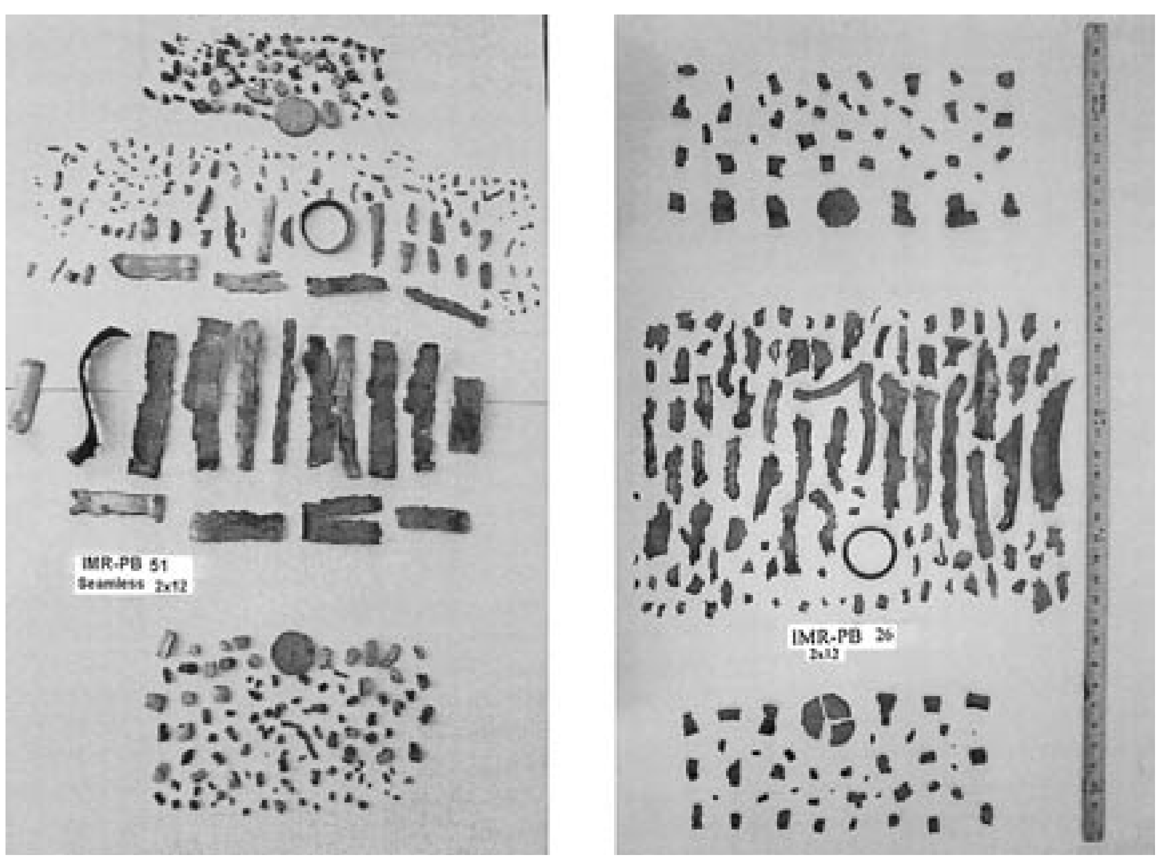


FIG. 16—*Fragments of pipes filled with IMR-PB—seamless steel (left), seamed steel (right).*

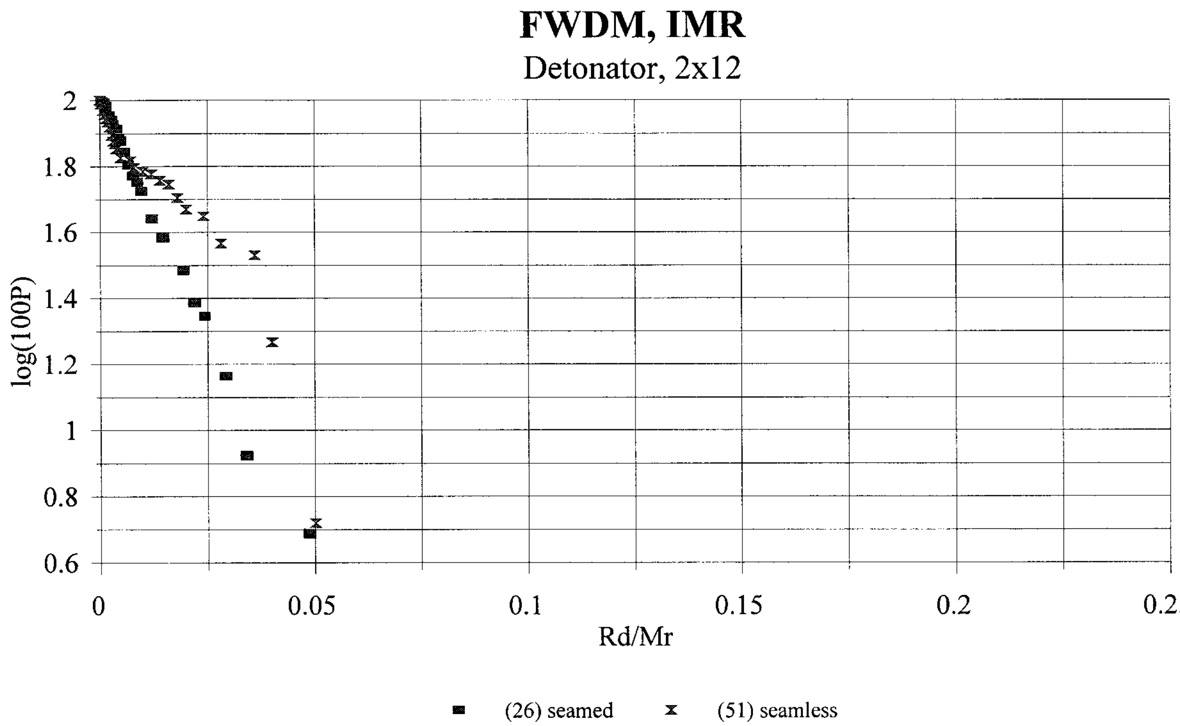


FIG. 17—*FWDM of fragments shown in Photo 16 (IMR-PB).*

faults throughout the pipe. Thus, the overall strength of the pipe matters. Low-energy materials, such as black powder, instigate a slow build-up of pressure throughout the pipe, and the pipe ruptures at the weakest point. Although the seamless pipe no longer has a weakness at the weld, the pipe/cap interface is still relatively weak; thus, the failure pattern does not change dramatically with the low-energy filler.

When PVC (polyvinylchloride) was the casing for black powder, the number of fragments increased tenfold over metal. This result would be expected for the weaker casing material, and, accordingly, the numerical evaluators are much larger than for the steel case. Furthermore, the PVC fragments exhibited a color change from white to orange/brown, indicating a chemical reaction between the powder and the PVC pipe. Bullseye, when exploded in PVC, did not discolor but melted the pipe. That the black powder would fracture the PVC, while the Bullseye would melt it is somewhat surprising. We suspect this is due to the speed of sound in PVC more closely matching the slowly burning black powder.

### *Effects of Device Orientation (Vertical vs. Horizontal) on Fragmentation*

Most pipe bombs (47) were placed in an upright position, with the bottom end cap buried in sand or Grit-o-Cob® and the detonator threaded through a hole in the upper end cap. A few pipes were placed horizontally with the initiator inserted through one end cap. Both with Red Dot and Bullseye, full pipes placed vertically (Red Dot 15, 17, 22 or Bullseye 6, 25) versus horizontally (Red Dot 48 or Bullseye 56) produced about the same number of pipe fragments, although the horizontal pipes produced many more end cap pieces (Fig. 20). In these cases, the FWDM slope was useful; it also indicated that the bombs exhibited the same power whether they were vertical or horizontal (Table 5). Half-full pipes were also compared in the vertical versus horizontal configuration. The results were not as clear as for the full pipes. Half a pipe of Red Dot in an upright pipe (46) gave an FWDM slope similar to horizontal pipe 53 (Figs. 21, 22). On the other hand, horizontal pipes 45 and 53 half-full of Red Dot should have been identical; the results were certainly not, possibly because it is difficult to reproducibly configure the powder in the pipe. Although the initial data suggests no real difference in the power of full vertical versus horizontal pipes, more tests are needed, especially of the low-energy fillers. It is obvious that in studying the partially full, horizontal pipe bomb, care is needed in duplicating initiator placement relative to the filler. All pipes were initiated from one end. The effect of initiating a vertical pipe from the bottom and a horizontal pipe from the center also needs to be examined.

### *Effects of the Amount of Fill on Fragmentation*

For vertical pipes with Red Dot, the full pipes (15,17,22) exhibited roughly the same number of fragments and the FWDM slope as the half-filled pipe (46) (Fig. 21, Table 5). Similar FWDM slopes were observed for horizontal pipes of Bullseye full versus three-quarters full; half-full pipes gave shallower slopes (Figs. 23, 24) (Table 5). For Red Dot, a fairly complete series was run in the horizontal position. No dramatic change in the FWDM slope was observed until the pipe was less than one quarter full. Even at 1/8 full there was some fragmentation (Fig. 25). It is expected that the percent of fullness required for pipe bomb performance will vary dramatically with the energy of the filler. For this reason tests are needed on each type of filler, and they should be linked with the orientation of the pipe and initiator.

### *Visual Observations*

Not only was explosive power observed in the number and size of the pipe fragments, but the visual appearance of each fragment

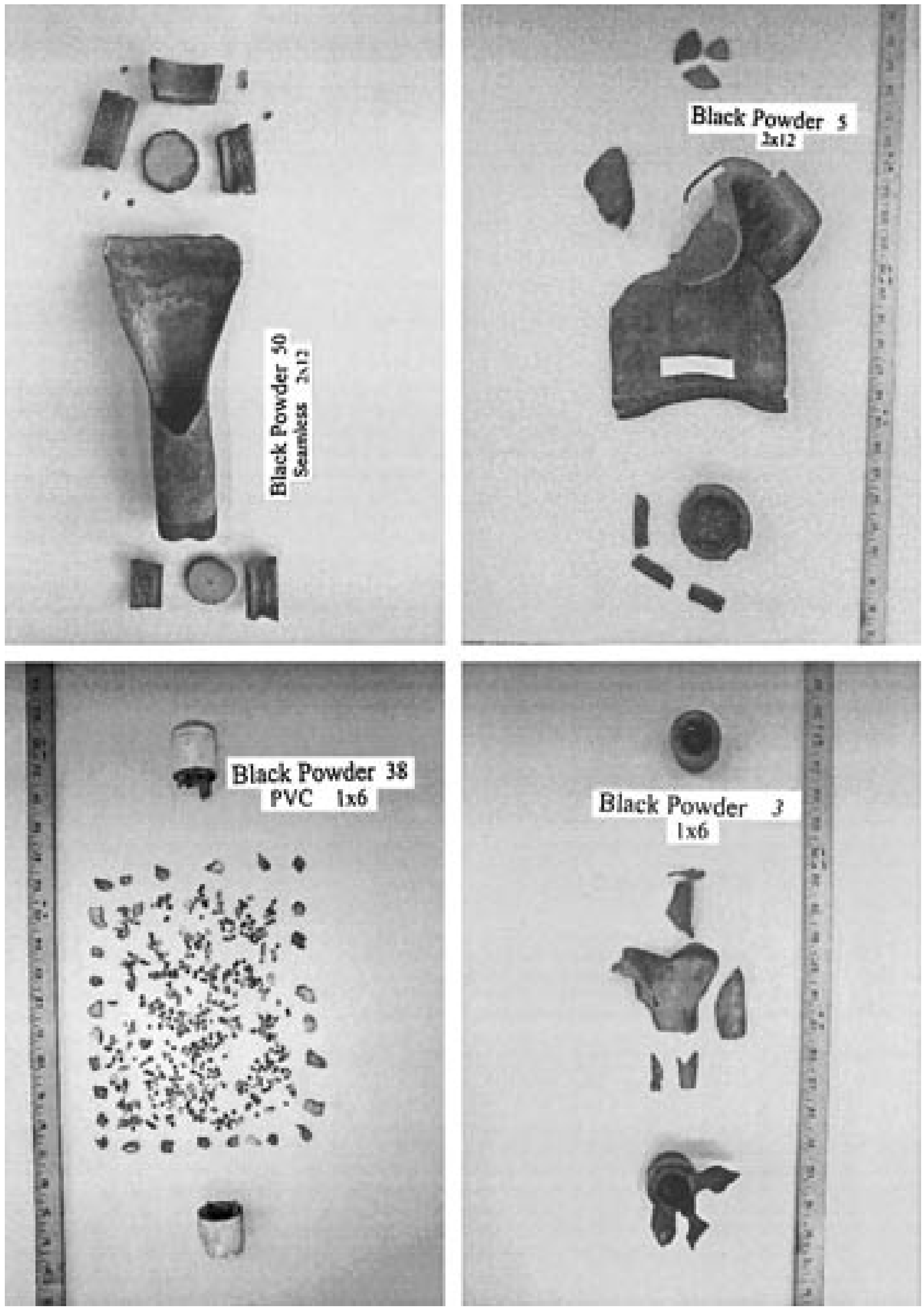


FIG. 18—*Fragments of pipes filled with black powder, clockwise from upper left—seamless (2" × 12") seamed (2" × 12"), seamed (1 × 6), PVC (1 × 6).*

reflected the explosive power of the device (5). Filler initiating low-energy events produced irregularly shaped fragments where the length to width ratio (L/W) was less than five. Higher-energy events produced strips where L/W was typically greater than ten. The irregular pieces produced by low-energy events were often bent and torn, while the strips produced by higher energy events were generally almost flat. Further evidence of the IED power was indicated by the appearance of the fragment edges. Low-energy fillers produced fracture edges which were about 90° to the center of the pipe. High-energy events produced fractures with sharp razor-like 45° edges (6). Observations under an optical microscope indicated the grain boundaries were significantly elongated with the high-energy fillers (7). Scanning electron microscopy (SEM) magnification of fragment surfaces indicated that the high-energy events produced smooth surfaces, while low-energy events produced a rough, textured morphology. Ordering the explosive power of the IED by the morphology of the surface compares reasonably well with the ordering suggested by total fragmentation (7).

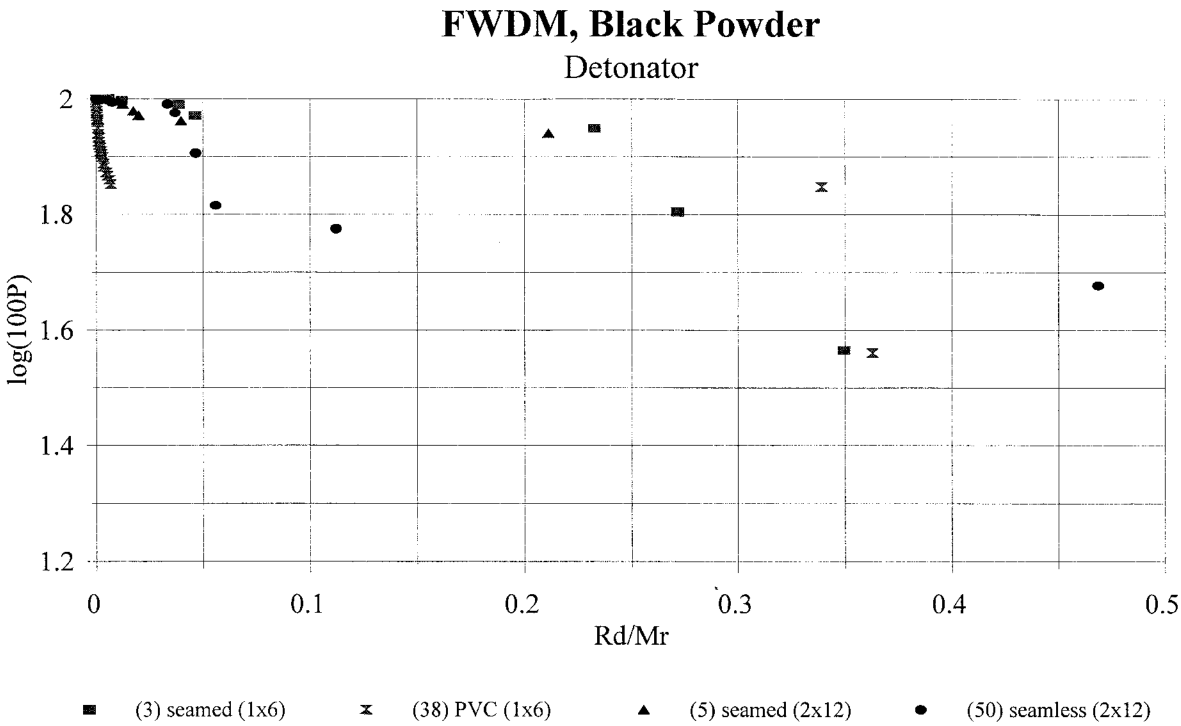


FIG. 19—*FWDM of fragments shown in Photo 18 (black powder).*

TABLE 5—*Effect of percent fill and pipe orientation.*

| | Red Dot (0.52 g/cc) | | % Recovery | Fragments Total | Pipe | Cap | FWDM Slope |
|---|---|---|---|---|---|---|---|
| 15 | vertical | Full | 72 | 118 | 54 | 63 | 13 |
| 17 | vertical | Full | 82 | 191 | 99 | 74 | 27 |
| 22 | vertical | Full | 86 | 210 | 125 | 92 | 27 |
| 46 | vertical | 1/2 | 96 | 257 | 122 | 135 | 13 |
| 54 | horizontal | 1/8 | 99 | 6 | 1 | 5 | 0.8 |
| 55 | horizontal | 1/4 | 98 | 157 | 9 | 148 | 10 |
| 53 | horizontal | 1/2 | 96 | 415 | 87 | 328 | 8.0 |
| 45 | horizontal | 1/2 | 93 | 18 | 6 | 12 | 2.6 |
| 47 | horizontal | 3/4 | 89 | 299 | 85 | 214 | 13 |
| 48 | horizontal | Full | 99 | 710 | 110 | 600 | 15 |
| | Bullseye (0.70 g/cc) | | | | | | |
| 56 | horizontal* | Full | 87 | 614 | 149 | 465 | 27 |
| 52 | horizontal* | 3/4 | 96 | 623 | 158 | 473 | 15 |
| 41 | horizontal* | 1/2 | 92 | 701 | 205 | 496 | 15 |
| 40 | vertical* | 1/2 | 94 | 558 | 168 | 390 | 47 |
| 6 | vertical | Full | 65 | 221 | 134 | 87 | 31 |
| 25 | vertical | Full | 74 | 258 | 166 | 91 | 45 |

Most pipes are galvanized steel welded pipes are 2 in. × 12 in.
* Pipes are 1.5 in. × 12 in. All pipes had detonator in one end.

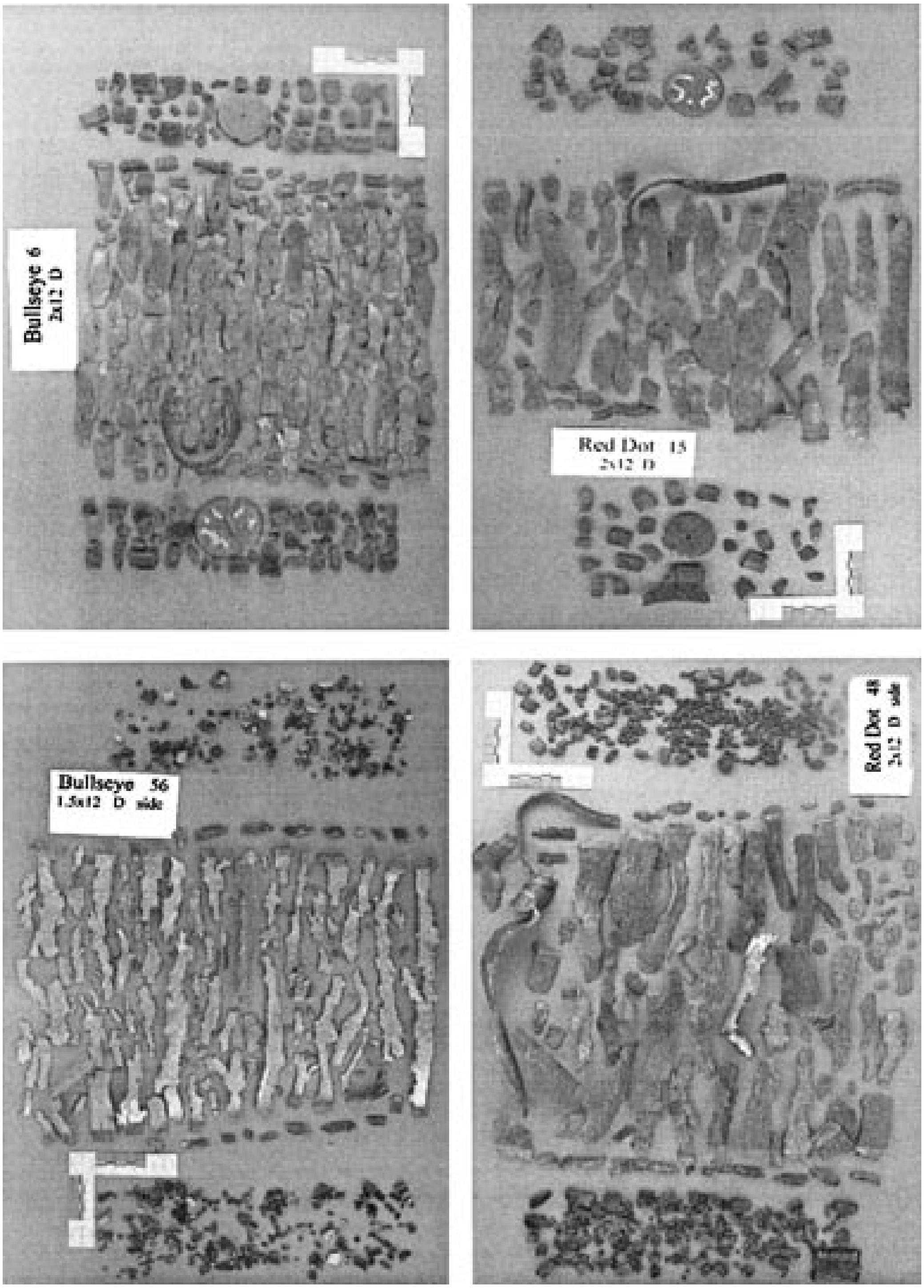


FIG. 20—*Vertical and horizontal pipes of Red Dot and Bullseye (Top pipes vertical; bottom pipes horizontal).*

## Discussion

In a slow burning event, where the velocity of burning front is much less than sound speed in both the propellant and the pipe, the pressure inside the pipe is uniform and rises as the amount of propellant burnt increases with time. When the total pressure rise exceeds the yield strength of the pipe material, the pipe will fail at the weakest point, usually the seam or end caps. A schedule 40 pipe is rated to withstand 700 psi (1 in.) or 1000 psi (2 in.) hydrostatic pressure (8). Alternatively, the energetic material may form a plug ahead of the burn front, causing a local pressure rise and rupture at that location. In either case, the pipe fragments will be large. Such were the type of events observed using black powder or WC-870.

Depending on the chemical nature of the energetic filler and the size and confinement of the system, the burning front may accelerate and transit from deflagration to detonation (DDT). If the material undergoes DDT, the detonation wave will propagate faster than the sound speed in either the pipe or the propellant. A detonation

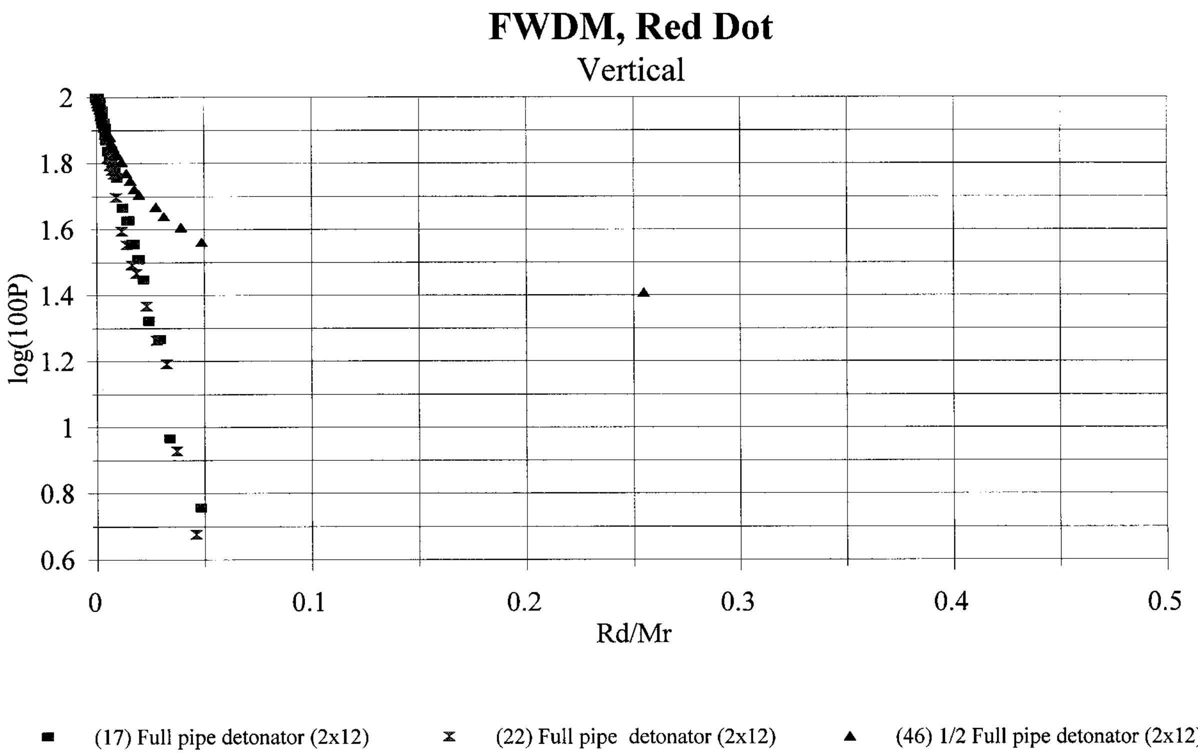


FIG. 21—*FWDM of fragments of 2 in. × 12 in. pipes (vertical) with various amounts of Red Dot.*

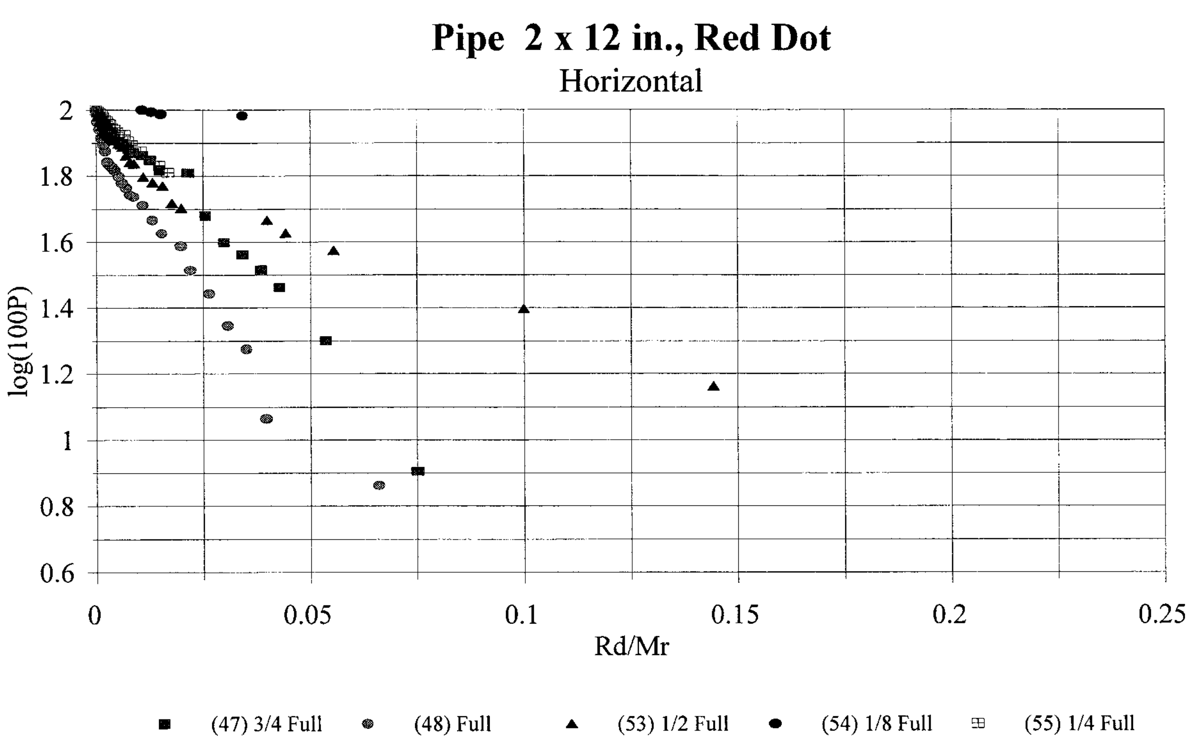


FIG. 22—*FWDM of fragments of 2 in. × 12 in. pipes (horizontal) with various amounts of Red Dot.*

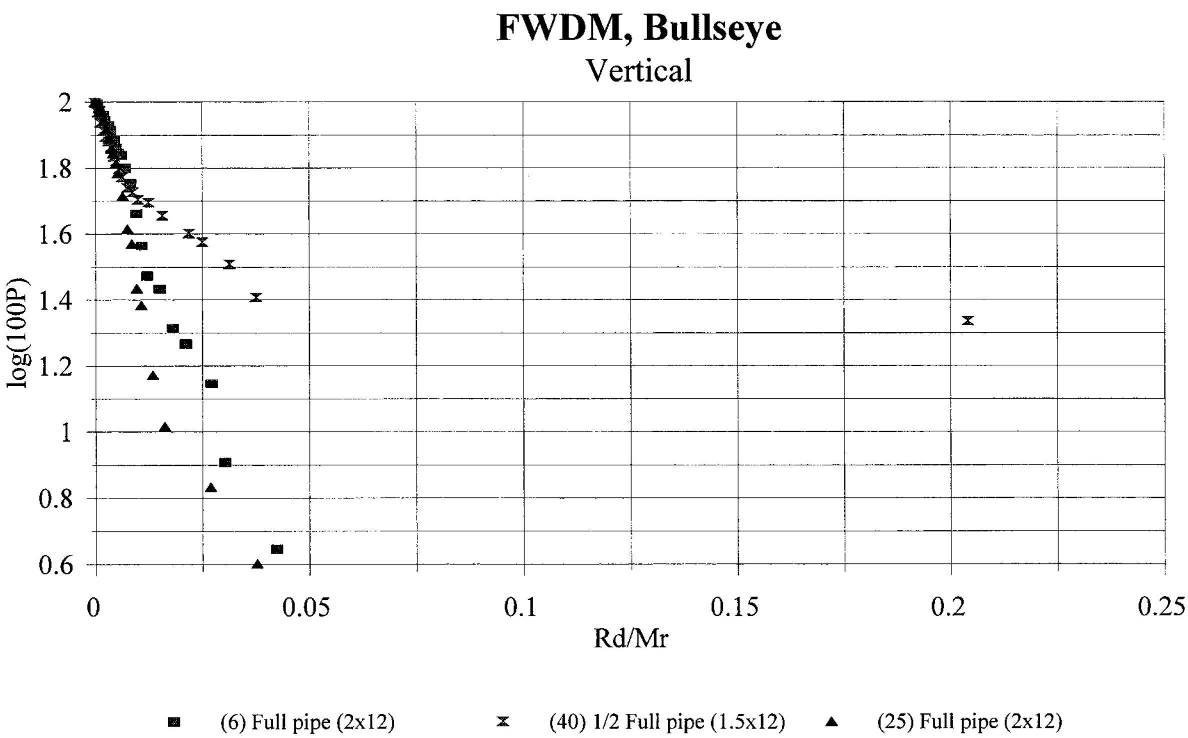


FIG. 23—*FWDM of fragments of 2 in. × 12 in. pipes (vertical) with various amounts Bullseye.*

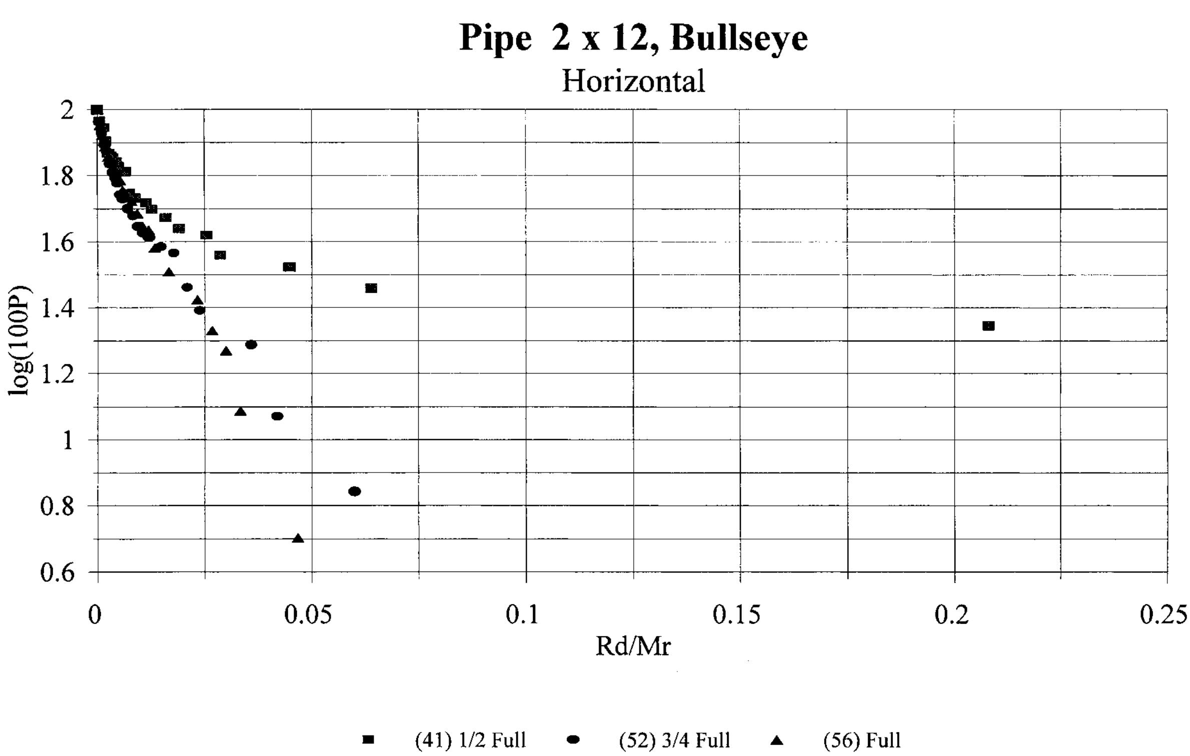


FIG. 24—*FWDM of fragments of 2 in. × 12 in. pipes (horizontal) with various amounts Bullseye.*

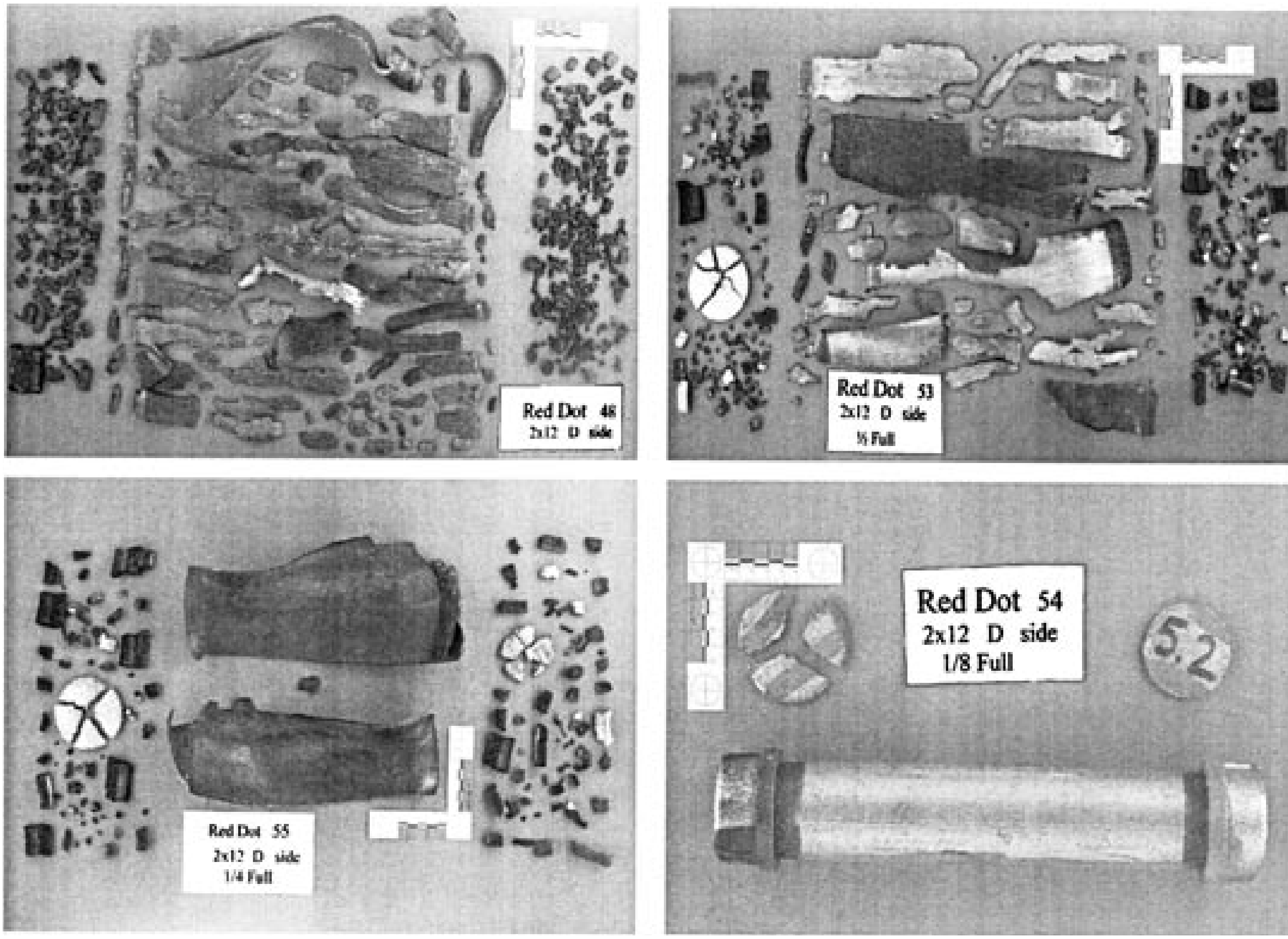


FIG. 25—*Fragments of pipes with various amounts of Red Dot (clockwise from upper left—full, 1/2 full, 1/8, and 1/4 full).*

rate of 6000 to 8000 m/sec (20 000 to 26 000 ft/sec) is typical for condensed high explosive (9). The detonation pressure is so high that the pipe fragments into tiny pieces as the detonation moves through the propellant and the pipe. Since the detonation wave moves through the pipe before the pipe or the material senses its approach, pressure build-up cannot be measured. It rises instantaneously with the detonation front, and complete fragmentation of the pipe occurs. In between the two limits of slow burn and detonation, the effect depends on the relation of burn rate to the sound speeds in the energetic material and in the pipe. We term this intermediate stage "medium-energy" although this is not a term to be found elsewhere. It is the medium-energy event, not quite detonation, that many of the high-energy fillers, such as Red Dot, experience. We rate the event just short of a detonation because the fragmentation is substantially less than that observed with nitromethane (Figs. 26, 27).

In judging the violence of an event, the number and size of pipe fragmentation and the appearance of the fragments can be used. Fragment Weight Distribution Maps (FWDM) were found to be reproducible and relatively insensitive to percentage recovery and to the size of the pipe. High or medium-energy events which produced lots of small fragments were recognizable by steep slopes; low-energy events, which formed few fragments, plotted shallow slopes.

Observations of the appearance of pipe fragments showed three types of fractures, listed below in order of observations for least to most violent events.

*Type 1*—Pipe is split open on the seam, with little damage. This is the result of an extremely low-energy event (Fig. 2, 28).

*Type 2*—Pipe is split into a few, irregular pieces, usually with edges of the pieces showing a break perpendicular to the center of the pipe. Pieces are often bent or torn, and some sections show bulging. If pipe fragments resemble strips, those by the pipe seam are the widest. This type of fragmentation is the result of a low-energy event (Fig. 2 black powder with squib).

*Type 3*—Pipe is split into long strips, close to full length of pipe. The strips on either side of the seam are usually the longest. On a Type 2 fracture, these seam-side pieces are usually the widest. In a Type 3 fracture, most strips are the same width with sharp 45° edges (Fig. 28). It is unusual that both sets of threads are present. Often one thread end is bent 180° back on itself and the other is missing. Type 3 fragmentation results from a medium to high-energy event. It is thought that a truly high-energy event should not result in metal strips, but rather in tiny pieces of pipe remaining; however, even nitromethane produces a fair number of metal strips (Fig. 26).

We summarize the pipe fragment damage by relating the burn (or detonation) rate of the energetic material to the speed at which the elastic deformation wave can travel in the pipe.

*Low-energy*: At a burn rate of 500 m/s (1600 ft/s), much less than the rate the elastic wave travels in the pipe, the pipe only partially splits because it breaks open releasing the gas before the crack propagates. Black powder is reported to have a burn rate of 500 m/s.[3]

*Medium-energy*: At a burn rate of 4000 m/s (13 000 ft/s), the crack begins at several defects and moves along the pipe toward each other. The results are strips of pipe with little notches.

*High-energy*: At a burn rate of 5000 m/s (16 000 ft/s), the pressure on the pipe is essentially the same throughout. The pipe fails at both big and little defects.

## Conclusions

Perhaps the most surprising conclusion is the reproducibility in fragmentation between identically prepared pipe bombs. Figures 1–3 dramatically illustrate this effect. Another noticeable point is that although six to eight formulations were examined, the fragmentation patterns can be categorized as from low-energy propellants (black powder and WC 870) or from high-energy propellants (Red Dot, IMR, Winchester, Bullseye). This differentiation was seen in the three numerical evaluators and in the visual appearance of the fragments. Of the evaluators examined, FWDM slopes were the most useful since they were independent of percent recovery, size of the device, and required no calibration shots. The low-energy materials had FWDM slopes between 0.2 to 2, while the high-energy materials had slopes between 20 to 60. The high-energy fillers appeared to be more sensitive to various parameters of the shot than the low-energy materials. This could have been because there was more room to observe changes in their very large FWDM slopes. However, there was no doubt that the high-energy materials performed significantly better when initiated by a detonator rather than by a squib. They may have performed slightly better when used in larger devices; clearly the high-energy fillers were

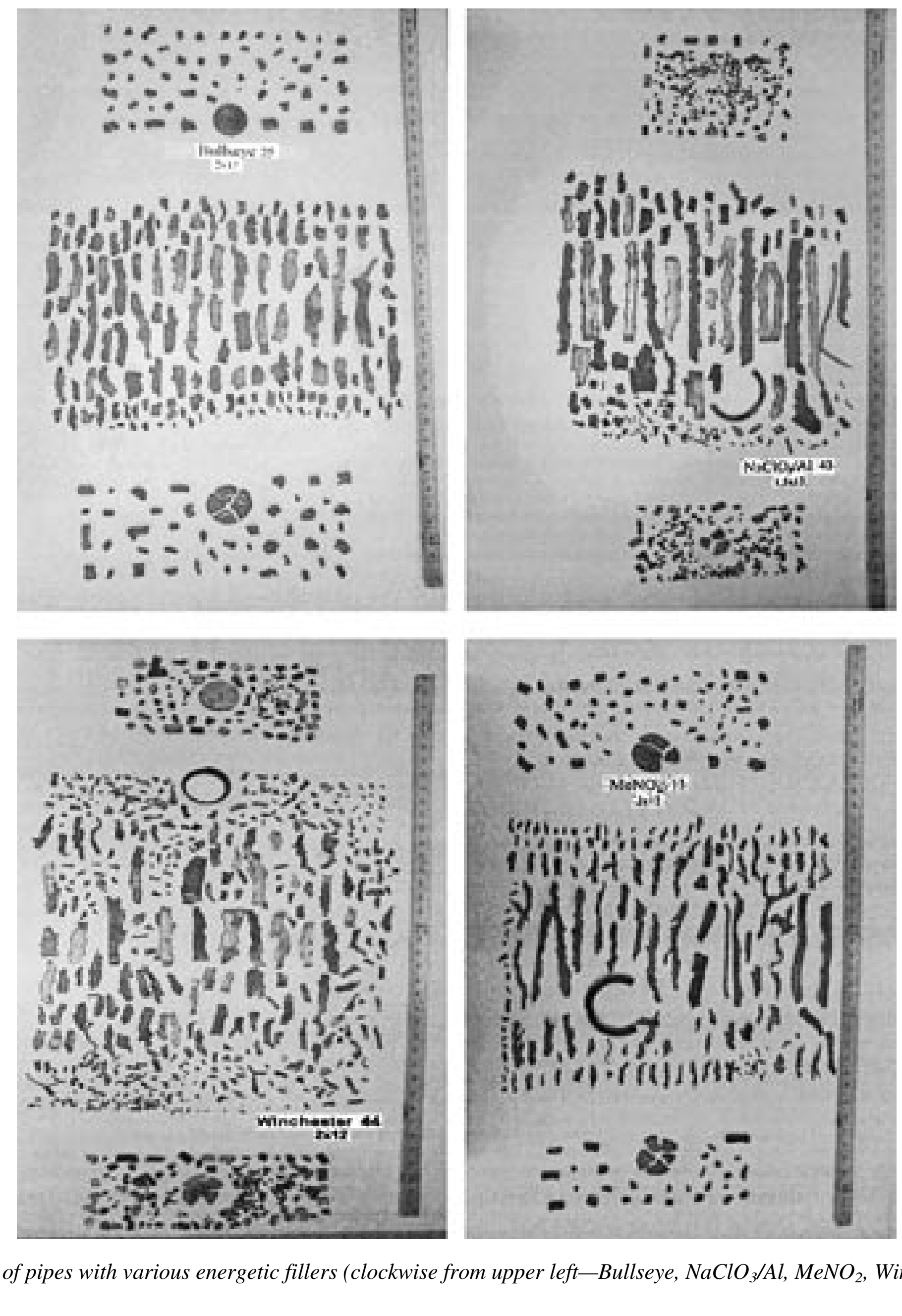


FIG. 26—*Fragments of pipes with various energetic fillers (clockwise from upper left—Bullseye, $NaClO_3$/Al, $MeNO_2$, Winchester Action Pistol).*

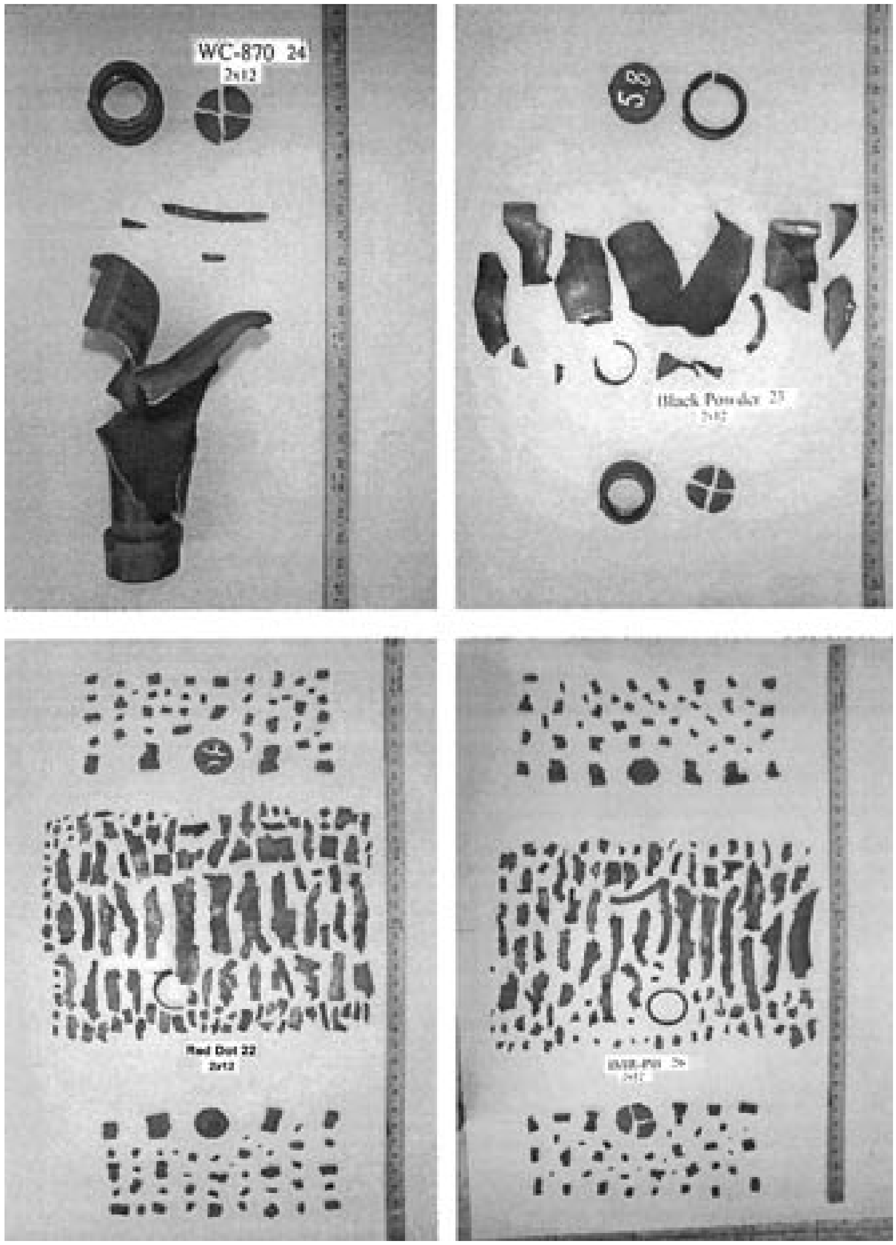


FIG. 27—*Fragments of pipes with various energetic fillers (clockwise from upper left—WC-870, black powder, IMR-PB, Red Dot).*

more sensitive to the type of casing, although the data is inconclusive. Black powder shattered and discolored PVC, while Bullseye melted it. The high-energy materials pulverized the end caps of the seamless steel pipes but left wide strips of pipe, whereas they produced small, narrow strips of the seamed pipe and broke its end caps into only a few pieces. Increasing the strength of the casing by using seamless rather than welded pipes had less of an effect on the low-energy materials than on the high-energy ones. This trend is surprising because it is well-known that high explosives are less sensitive to the degree of confinement than low explosives. We assume that the trend observed herein only holds when comparing low explosive against each other. Very low-energy materials, like black powder, instigate rupture of the pipe at the weakest point, which is usually the pipe/cap interface.

Insufficient studies were performed comparing horizontal versus vertical and partially full pipes to make more than tentative conclusions. It appears that vertical versus horizontal placement has little effect on full pipes, and that partially full pipes, if containing a sufficiently powerful propellant, may perform as well as full ones.

In real bomb scenes, fragments are on roofs, in ponds, or otherwise invisible. Full recovery may not be possible. The chemical residue may have been washed off with a fire hose or contaminated with gasoline, anti-freeze, or body fluids. This study demonstrates the possibility that, even in circumstances where chemical residue cannot be found, sufficient evidence is present in the pipe fragments to identify the nature of the energetic filler.

## Future Work

More tests are needed to clarify the effects of pipe orientation or degree of fill. All pipes were initiated from one end; the effect of initiating a vertical pipe from the bottom or a horizontal pipe from the center needs to be examined. Of major interest is the effect of the sand or Grit-o-Corn® filled barrels on fragmentation. New tests will include

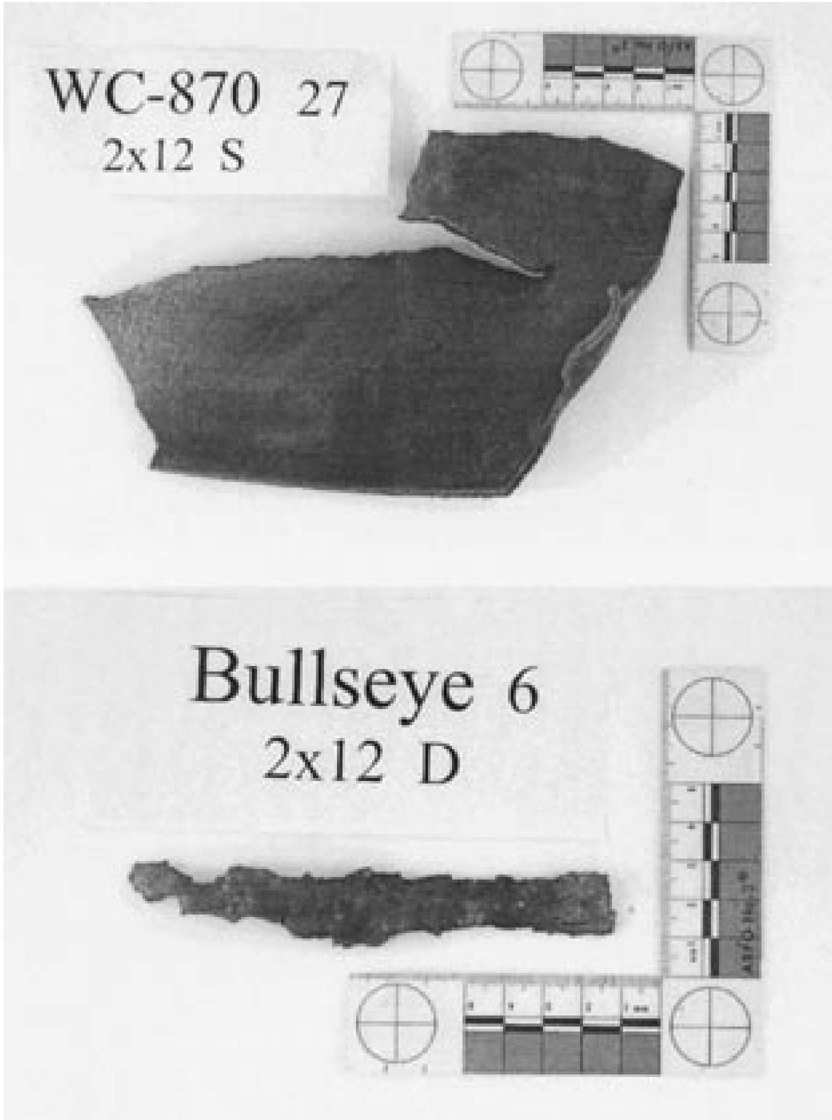


FIG. 28—*Photos of single fragments illustrating 45° and 90° edges.*

free-field studies. We would like to expand the basic study herein to include a wider range of powder densities and pipe materials.

*Acknowledgments*

The authors thank TSWG for funding this project through the Office of Naval Research and the URI Forensic Science Partnership for supplemental funding. The authors also thank Dr. Otto Gregory of University of Rhode Island (URI) for helpful discussions and Norman Stamm of Ares Inc. for technical support.

## References

1. Bureau of Alcohol, Tobacco and Firearms. 1997 Arson and Explosives Incidents Report. Washington, DC: Dept. of Treasury; 1997.
2. Bender EC. Analysis of low explosives. In: Beveridge A, editor, Forensic investigation of explosives. London: Taylor & Francis, 1998; 343–87.
3. Walsh B. The influence of geometry on the natural fragmentation of steel cylinders. Maribyrnong, Victoria, Australia: Australian Defence Scientific Service Defence Standard Lab, Jan. 1973; Report 533.
4. Zaker TA. Fragment and debris hazards TC12. Washington, DC: DoD Explosives Safety Board, July 1975; Report AD-A013 634.
5. Tardif HP, Sterling TS. Explosively produced fractures and fragments in forensic investigations. J Forensic Sci 1967;12(3):247–72.
6. Ryder DA. Failure analysis and prevention. In: American Society of Metals, Metals Handbook 9th ed, Vol. 11: Philadelphia: ASM, 1986;1–101.
7. Gregory O, Platek M, Cuminski C, Oxley J, Smith J, Resende E. Steel deformation under high temperature, high pressure events. Materials characterization. In press.
8. ASTM. Standard specification for pipe, steel, black and hot-dipped, zinc-coated, welded and seamless ASTM Standard A 53–93A. Annual Book of ASTM Standards. Philadelphia; ASTM, July 1993.
9. Oxley JC. The chemistry of explosives. In: Walters B, Zukas J, editors. Explosives effects and applications. New York: Springer, 1998; Ch. 5.

Additional information and reprint requests:
Jimmie C. Oxley
Associate Professor
University of Rhode Island
URI Chemistry, 51 Lower College Road
Kingston, RI 02881
Tel: 401-874-2103
Fax: 401-874-2103